NTNU – Trondheim
Norwegian University of
Science and Technology

Friction reduction by using nanoparticles in oil-based mud

Elshan Jabrayilov

Petroleum Engineering
Submission date: July 2014
Supervisor: Sigbjørn Sangesland, IPT

Norwegian University of Science and Technology
Department of Petroleum Engineering and Applied Geophysics

DEDICATION

This thesis is dedicated to my father, Ramiz Jabrayilov, my mother, Naila Jabrayilova, my two brothers, Elnur Jabrayilov and Jeyhun Jabrayilov and my lovely nephew, Farid Jabrayilzadeh.

Summary

Nowadays, increasing demand on petroleum resources and depletion of easy accessible reservoirs result in exploration of challenging reservoirs. Drilling of deeper reservoirs is an important part of this challenge where increasing the well depth and harsh drilling circumstances arises torque and drag problems and "smart drilling fluids" are required to overcome such problems. These fluids can be obtained by using of some nano-materials to improve the tasks and features of drilling fluids. Use of the nanoparticles are promising and adding them into the drilling fluids can solve some problems during drilling such as lost circulation, pipe sticking, thermal instability, torque and drag and etc. In this work, improvement of lubrication behavior of drilling fluids are mainly investigated by adding nanoparticles into the oil-based mud (OBM).

Tribological and rheological experiments were conducted to examine reduced friction and rheology of the mud by using titania and silica nanoparticles as an additive. Additionally, silica microparticles were also tested to compare with nanoparticles and to highlight the advantages of using drilling fluids with the nano-scale additive. Different particle concentrations were tested at the different temperatures to observe the effect of nanoparticle added fluids on rheological and tribological properties. The main purpose of this work is to determine right type of nanoparticles with optimum concentrations.

In this thesis, rheological and tribological measurements were conducted on a modular compact rheometer (MCR). Afterwards, only tribological measurement was performed on standardized in-on-disk apparatus to validate the results acquired from MCR. The tribology experiments with the MCR and pin-on-disk (POD) apparatus were performed using rotational ball sliding on sample plates and disks, accordingly. While viscometer measurements with the MCR were done based on the function of the Fann viscometer.

According to the experimental results, titania and silica added nanoparticles showed good reduced friction properties. Especially, silica nanoparticle added fluids with the concentration of 0.25 weight% reduced friction coefficient by 47% at the temperature of 50°C. It is also found that silica nanoparticles are more effective in reducing the friction coefficient when it is compared to silica micro-particles. Additionally, coupling effect theory between temperature

and nanoparticles was prove with addition of nanoparticles (NPs) to the OBM. As further study, optical 3D confocal microscope was used and OBM was found better lubrication than water-based mud (WBM) as a drilling fluid.

Acknowledgement

This thesis work was completed at the Norwegian University of Science and Technology (NTNU), in the Department of Petroleum Engineering and Applied Geophysics. The thesis is the final product of TPG4920 (Petroleum Engineering, Master's Thesis) and it corresponds to 30 ECTS. The objective of the thesis was to investigate friction reduction by adding of nanoparticles to OBM.

It could not have been possible to complete this thesis without the help and supports from special people. First of all, I am very thankful to my supervisor, Sigbjørn Sangesland, for letting me choose and work on such an interesting topic. He was always kind, supportive and helpful during the thesis work. Special thank goes to my another supervisor, Pål Skalle, for his valuable help in the drilling fluid part. I wish to thank my co-supervisor, Jianying He, who gave me wise advices and suggestions throughout my thesis work.

I wish to express my regards to Roger Overå for his valuable assistance working with modular compact rheometer in IPT laboratory. I also wish to acknowledge Cristian Torres Rodríguez for the guidance and help in tribology lab at NTNU.

Thanks also to my friends, Farad Kambayi and Anwar Sufi, who were so supportive and generous, they always kept my moral high and motivated me to complete my thesis work. Last but not least, I would like to be grateful to my parents and my friends both in Azerbaijan and Norway for their support and faith in me.

Trondheim, July 2014

Elshan Jabrayilov

Table of Contents

List of Figures

List of Tables

Abbreviation

NP	**N**ano**p**article
EOR	**E**nhanced **O**il **R**ecovery
OBM	**O**il-**B**ased **M**ud
WBM	**W**ater-**B**ased **M**ud
3D	**T**hree **D**imensional
MCR	**M**odular **C**ompact **R**heometer
ERD	**E**xtended **R**each **D**rilling
HPHT	**H**igh **P**ressure **H**igh **T**emperature
POD	**P**in-**O**n-**D**isk
GBM	**G**as-**B**ased **M**ud
NCS	**N**orwegian **C**ontinental **S**helf
ROP	**R**ate **o**f **P**enetration
NTNU	**N**orwegian **U**niversity of **S**cience and **T**echnology
RPM	**R**evolution **p**er **M**inute

Nomenclature

τ	Shear Stress
γ	Shear Rate
τ_0	Yield Stress
μ	Viscosity
μ_{pl}	Plastic Viscosity
n	Flow Behavior Index
K	Consistency Index
A	Area
μ	Friction Factor/Coefficient
d	Wear Scar Diameter
r	Radius
V	Volume
R_w	Wear track radius
F_L	Normal Load
F_R	Frictional Force
α	Deflection Angle
M	Torque
v	Velocity
S	Distance
ϕ	Displacement Angle
n	Revolution per Minute
ω	Angular Velocity
L	Length
ρ	Density
W_{NP}	Weight of Nanoparticle
C	Concentration

1. Introduction

In extended and horizontal well drilling, one of the key factors that limits the well length is the torque and drag between the drillstring and wellbore. This results in decreased drainage efficiency of oil reservoirs. High friction can cause increase in hookload during tripping out which leads to reduction in the equipment life and essentially a decrease in the well length. There are several innovative mud systems that have been applied to combat these problems in completion and drilling engineering. One of these innovative mud systems is nanofluid where nanoparticles (NP) are added to the drilling fluid [1].

Application of nanotechnology in the oil industry, especially for enhanced oil recovery (EOR) and drilling can be beneficial in the wettability alteration, in forming binders for sand consolidation and in drag reduction [2] [3].

There have been a large number of papers describing and investigating tribological properties of lubricants with the addition of nanoparticles where significant reduction in friction and wear was reached. The friction reduction and lubrication behaviors depend on the properties of nanoparticles in terms of the shape, the size and the concentration in the tested fluids. The size of the nanoparticles generally ranges between 1-120 nm [4].

This thesis is based on the thesis work performed by C. Jahns in 2014: "Friction reduction by using Nano-Fluids in Drilling". In that thesis work, tribological measurements were performed with nanoparticles contained water-based mud (WBM) to measure the friction and lubrication properties of the WBM. Silica, titania and alumina were the nanoparticles used in the experimental phase. Based on the results of the experiments, alumina showed limited efficiency on lubrication behavior, whereas, titania and silica nanoparticles showed significant reduction in friction between steel surfaces. Since WBM is more environmental friendly it is usually the preferred drilling fluid. However, with increasing wellbore depth, torque and drag problems arise and, the ability to use WBM is decreased and as a result, oil-based mud (OBM) is used to drill further.

Therefore, the main motivation of this work is to investigate tribological properties of OBM with and without nanoparticles, called silica and titania with 40-60 nm particle size. In

addition, micro-silica with 300 nm particle size were added to the drilling fluid to compare with the NPs contained OBM.

Further investigations were performed using an optical 3D confocal microscope to interpret the feasible mechanisms of wear and lubrication with tested nanoparticles and to extract some parameters for loss volume calculations in the disk. Moreover, the effect of temperature on the rheology of tested fluids were investigated.

Tribology measurements were performed by using a modular compact rheometer (MCR) and pin-on-disk (POD) apparatus. Firstly, wear and friction properties were measured by MCR with the tribology measuring cell and then based on the results of the MCR apparatus tribology tests were planned for the pin-on-disk (POD) apparatus. Rheological behavior of the tested fluids were examined with the modification of MCR.

The main purpose of this thesis is to investigate reduction in wear and friction, and increase in lubrication behavior of the OBM with the optimum concentration of different types of nanoparticles in a specific temperature.

The first step is to conduct literature review about the basics of the tribology and rheology as well as more main aspects related to this work. Thereafter, planning an experimental investigations, installation and procedures of MCR and pin-on-disk (POD) apparatus will be presented. Finally, the results will be outlined and importance of using nanoparticles in the drilling fluids will be mentioned.

2. Theory

A drilling fluid, sometimes referred to as the drilling mud, is a fluid used in a drilling operation. It is pumped down from the surface through the drill string and the drilling bit and back to the surface through the annular space [5]. Figure 2.1 illustrates the drilling mud circulation process.

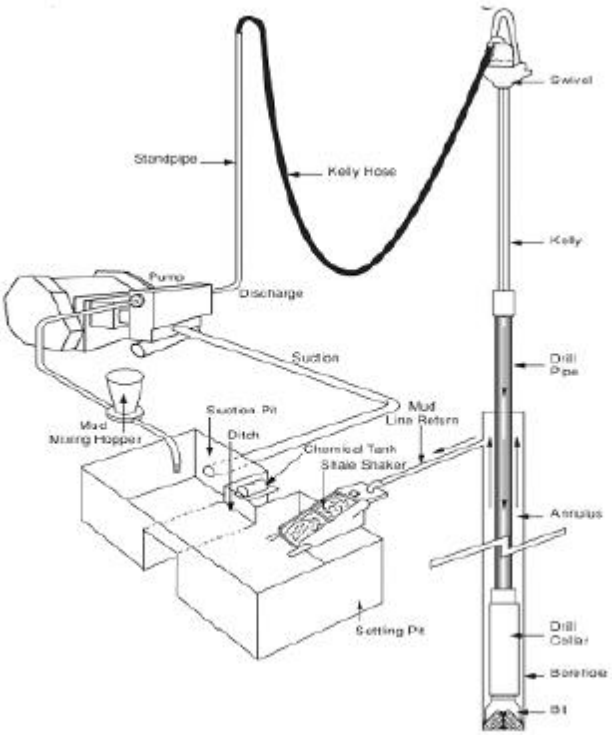

Figure 2.1: Drilling fluid circulation [6].

In order to drill the oil well successfully drilling mud must carry out several:

- to carry cuttings out of the hole,
- to maintain the hydrostatic pressure in the wellbore to drill ahead,
- to clean and cool the drill bit,
- to suspend cuttings when the circulation is immobile,
- to prevent formation damage,
- to give information from downhole to the surface,
- to prevent extreme mud loss by a forming filter cake and
- to reduce friction between the side of the hole and the drill string [5][7].

A drilling fluid is a complex mixture and contains different type of additives. The type and concentration of these additives depend on the type of drilling methods and reservoirs to be drilled. The drilling fluids can be widely classified as oil-based mud (OBM), water-based mud (WBM), synthetic-based mud (SBM), emulsions, air form fluids and so on [8]. Moreover, some additives and viscosifiers are added to the base fluid to obtain proper viscosity and some other parameters which help to fulfill drilling fluids' functions.

As mentioned in the work done by Amanullah et al., (2009) [9], "industry is looking for mechanically strong, physically small, chemically and thermally stable, biologically degradable, environmentally benign chemicals, polymers or natural products for designing smart fluids to use virtually in all areas of oil and gas exploration and exploitation." In the last decade nanotechnology was presented as a new concept which may have potential improvements in different fields. For example, applications of NPs as a new type of additive in the OBM has received remarkable interest and has inspired to more research and experimentation [10]. A more thorough description of nanoparticles can be found in section 2.3.

2.1. Basics of tribology

Extended reach drilling (ERD) is one of the important progress in drilling. One of the important factor is friction that plays a main role here, both related to the completion and the drilling stage of the well [11]. Basically friction is created when the elements move relative to each other and obtain drag force. Friction, wear and lubrication are the main part of science termed Tribology. The meaning of tribology comes from the Greek word 'tribos' which refers to the sliding or rubbing. The fundamental concept of the tribology is the best controlled friction and wear with a thin layer between the materials created by rolling, sliding and impacting bodies. There is nearly no limitation on the type of material which can form such a film. If the film is not provided then wearing process creates a substitute film. The purpose of tribology is either to provide optimum film for a specific application or to anticipate the series of events when rolling, sliding and impacting contact remained to create its own intervened film [12]. Tribological design and choice of materials play important roles in the drilling and completion operations. There are some parameters that have an effect on the tribological behavior [13]:

- size/shape/concentration/solidness of the particles,
- the forces used over the materials,

- wear modes,
- the time interval of contacted materials and
- type of fluids used in drilling.

In the following subsections tribological parameters such as wear and lubrication will be briefly outlined.

2.1.1. Wear modes

Wear is defined as a removal of material from one body when exposed to a contact and a relative motion with another body. These are the following primary wear modes [14]:

- Adhesive wear
- Abrasive wear
- Fretting corrosion
- Erosive wear and
- Fatigue wear [14].

Adhesive wear is characterized as a very serious type of wear and this wear is described as high wear rates and unstable friction factor. Abrasive wear happens when the harder material scratches the softer material and creates mass and volume loss on the softer material [12][14]. This type of wear is very important because sliding and impact movement is common during drilling [13]. Figure 2.2 illustrates different mechanisms of abrasive wear.

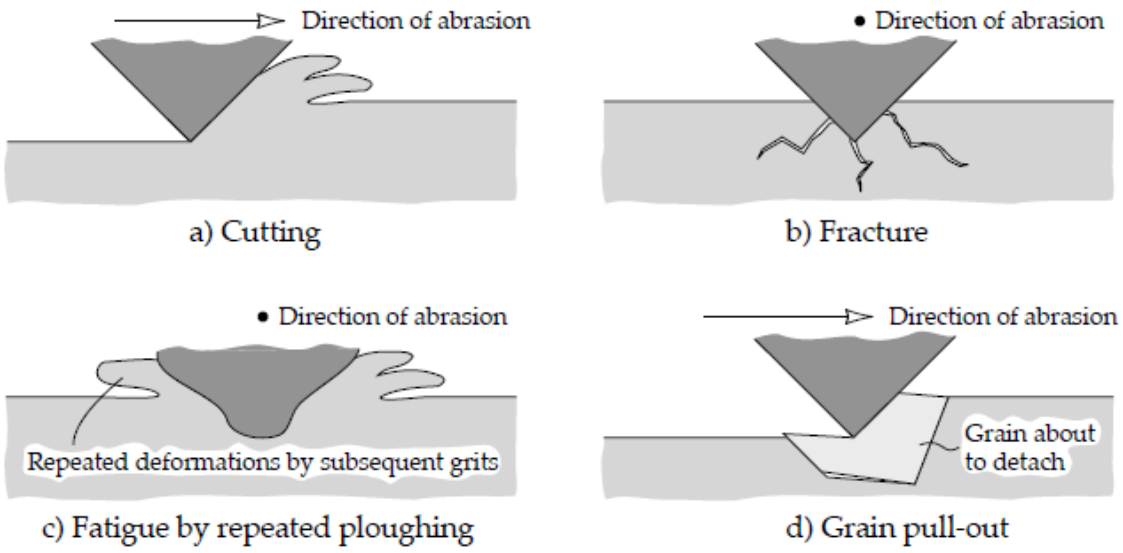

Figure 2.2: Abrasive wear mechanisms [12].

Fretting wear is characterized as a repetition of cyclical rubbing between two surfaces and this causes removal of material from either one or both surface in contact over an interval of time [14]. Erosive wear is described as an overly short sliding movement and is carried out during a short time frame. When the intervening films are partly active then milder types of wear take place and these are generally generated by fatigue process as a result of repletion of stresses under either rolling or sliding. This types of wear can be called fatigue wear. There is another types of wear called corrosive and oxidative wear. The basic characteristic of these types of wear is a concurrent chemical reaction between a corroding medium and the worn material. This wear is common term referring to any type of mechanical wear that is related to a chemical or corrosive process [12].

2.1.2. Lubrication

As outlined before when two bodies are in contact by sliding, rolling or separating with respect to each other friction force is generated at their interface in the opposite direction of their movement. This force is generally accompanied by wear which means removal of the material from either from one body or both of the contacting surfaces. The process that minimizes the wear and friction is called lubrication [15]. Oil viscosity plays primary role in the lubrication. Depending on the different types of oil have different lubrication effects. Additionally, oil viscosity is generally proportional to the temperature, pressure and shear rate and the thickness

of the oil film. It is obvious that more viscous oil can generate better lubrication effect. Thus, the film created between bodies can be thicker and a better separation in the contacted surfaces can be obtained. However, this is not always the case, thus more viscous oil requires more power to be sheared. As a result, more power and heat is created causing a substantial temperature increase in the surfaces which may result in the failure of the component. In general, oil viscosity is used to give optimum performance regarding the required temperature, since the viscosity is temperature dependent which means viscosity of different oils changes at different rates regarding temperature. The velocities of the operating surfaces also have an impact on the viscosity. For this reason, knowing the viscosity features of a lubricant is very important in designing and in the prognosis of the behavior of a lubricated system [12].

NPs are new type of additives added to the drilling fluids to improve lubrication effect and to reduce friction between the metal surface and the hole. More about the viscosity and other features of the drilling fluids and NPs will be discussed in the following sub-chapters.

2.2. Rheology of drilling fluids

Rheology is defined as the science of flow properties and the deformation of matter. Rheology of fluids measures viscosity, elasticity and yield point [16]. Basically, the deformation of fluids can be explained by two parallel separated plates regarding some distance as illustrated in Figure 2.3.

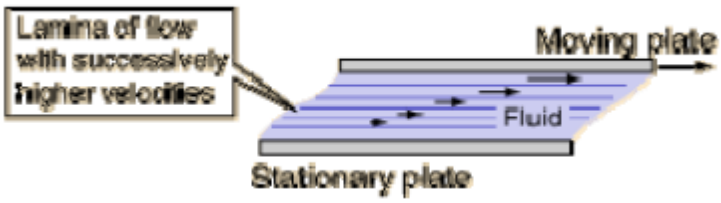

Figure 2.3: Fluid deformation by simple shear [17].

When an applied force (F), acting over an area (A), results in the sliding of the layers in relative to each other which causes resistance or frictional drag force in the opposite direction of these plates. This resistance is termed shear stress (τ) and it is expressed as following equation:

$$\tau = \frac{F}{A} \tag{2.1}$$

Shear rate (γ) is defined as the rate of change of velocity at which one layer of fluid passes over the adjacent layer. Sometimes, shear rate can be defined as velocity gradient and mathematically expresses as following equation:

$$\gamma = \frac{velocity\ difference}{distance} \tag{2.2}$$

Fluid behavior is defined according to the relationship between the shear stress and the shear rate. If the relationship between the shear stress and the shear rate is linear i.e. if the shear rate increases two times then shear stress will increase two times then this type of fluids is called Newtonian fluids. If the relationship between shear stress and shear rate is not linear i.e. if the shear stress does not increase in direct proportion to the shear rate then this type of fluids is called non-Newtonian fluids. In drilling, most of the drilling fluids follow non-Newtonian fluid characteristics [17].

2.2.1. Viscosity

Viscosity (μ) is a resistance of the fluid to flow. For Newtonian fluids the viscosity is defined as a ratio of shear stress to shear rate. Mathematically, the viscosity of the Newtonian fluids is:

$$\mu = \frac{\tau}{\gamma} \tag{2.3}$$

As described before, relationship between shear rate and shear stress is linear. So, for Newtonian fluids the viscosity is always constant and it is the only parameter required to characterize properties of the flow. Whereas, for the non-Newtonian ones, the dependency between shear stress and shear rate is not constant and is defined as the effective viscosity. The effective viscosity is low with high shear rates and vice versa. This phenomena is called shear thinning and this behavior of the drilling fluids is very desirable i.e. gel structure will be formed with low shear rates which leads to cuttings to be suspended in the mud and this gel is broken with increasing shear rates. This process helps to clean cuttings out of the hole [17]. Nowadays, the following non-Newtonian models are mostly applied to drilling fluids [16].

- Bingham plastic model,

- Power law model and
- Herschel and Bulkley model.

For Newtonian model one constant is enough to determine the model by using equation (2.3). The Bingham or the Power law model expresses the rheology of the simple fluid composition. 2 data points are required to determine the Bingham and the Power low models because of two unknowns in the equation. These unknowns can be found by using the following equation (2.4) and (2.6), respectively:

$$\tau = \tau_0 + \mu_{pl}\gamma \tag{2.4}$$

Where, μ_{pl} and τ_0 are the plastic viscosity and yield point (gel strength) of the fluid, respectively and μ_{pl} can be found by using equation (2.5):

$$\mu_{pl} = \frac{\tau_{600} - \tau_{300}}{\gamma_{600-}\gamma_{300}} \tag{2.5}$$

$$\tau = K\gamma^n \tag{2.6}$$

Where, K- consistency index, n - flow behavior index
The constants of Power low, n and K are found by the equation (2.7) and (2.8):

$$n = \frac{log\tau_{600} - log\tau_{300}}{log\gamma_{600-}log\gamma_{300}} \tag{2.7}$$

$$K = \frac{\tau}{\gamma^n} \tag{2.8}$$

In high pressure and high temperature (HPHT) conditions and in some other conditions such as the narrow pressure window is established high demand drilling fluids are required. Thus, complex fluid rheology model for instance Herschel Bulkley model is investigated. Because of the three unknown variables in the equation (2.9), three data points are required to define this model [16].

$$\tau = \tau_0 + K\gamma^n \tag{2.9}$$

The yield point can be assumed equal to 3 Pa or can be calculated graphically. The variable K can be calculated by equation (2.10) after obtaining n from the graph slope [16].

$$K = \frac{\tau_2 - \tau_0}{\gamma^n{}_2 - \gamma^n{}_0} \tag{2.10}$$

Figure 2.4 illustrates flow curves of fluids rheological models described above. In drilling, first, drilling fluid is prepared and plotted, then, proper rheological model is applied to the fluid to predict fluid properties in specific conditions.

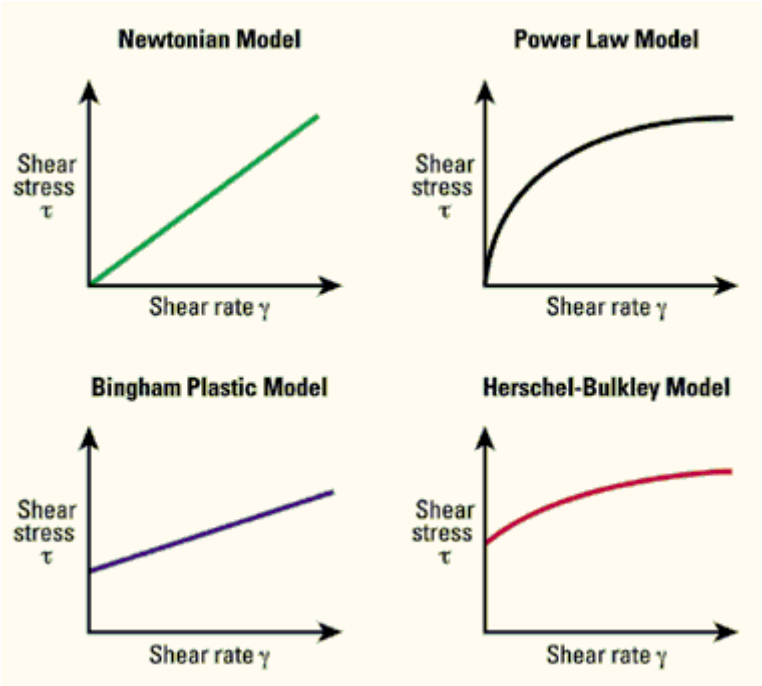

Figure 2.4: Rheological models of the fluids, modified after [18].

Every additive including NPs in the drilling fluids have their impact on the rheological behavior of the fluid. In this thesis, optimum particle concentration shall be found to reduce friction in the wellbore. For this reason, volume fraction of the NP have to be carefully analyzed to minimize their effect over viscosity [13].

2.3. Nanoparticles

Over last decade, application of nanotechnology in different industries such as electronics, medicine, biomaterials and renewable energy production has already brought new technological advances [2] . Due to the greater risk and high cost of adapting new technologies, the application of NPs is in its infancy in the petroleum industry. Based on the results in the

lab experiments and papers, nanotechnology can improve global recovery factor of oil and gas by 10% and application of nanotechnology in the petroleum industry is very expected in the near future [19][3].

Application of nanotechnology can revolutionize the behavior and characteristics of the additive by setting particle properties to accomplish particular operational, technical and environmental requirements. Since preparation some tailored made NPs by the nanotehcnological research can be promising step for the "smart fluids" development for EOR and drilling [9]. The diameter of the NPs are commonly in a range of 1 to 100 nm size, can have many special characteristics and can be created in various ways. These particles are great scientific point of interest which they can effectively bridge bulk material and molecular or atomic structures [19].

By adding of NPs, the properties of the base fluid can be tuned to the optimum level. Basically, these particles are in a suspension form in the liquid phase (oil, water or conventional fluid mixture) in the low volumetric fractions. Using the NPs in the design of such fluids are preferably inorganic with properties of no aggregation or dissolution in the liquid environment. Nano-based fluids can be designed to be compatible with reservoir fluids and they are environmentally friendly. Recent experiments already showed that these "smart fluids" can be promising in drilling by adding benefits such as advanced drag reduction, an alteration of wettability, binder for sand consolidations and reducing interfacial tension [3]. Furthermore, NPs contained fluids can be beneficial in some other drilling problems such as borehole instability, lost circulation, pipe sticking problems and gumbo and bit balling. To be relevant to this thesis work friction reduction between drill string and borehole shall be discussed.

2.3.1. Torque and drag

Nowadays, torque and drag problems are arisen rapidly while drilling by changing vertical and directional drilling to horizontal and extended reach drilling (ERD). The friction factor is the main component in the torque and drag which is created between the borehole wall and the drill string. One of the functions of the drilling fluids is to minimize the torque and drag problems. Macro and micro material-based drilling fluids have limited capacity to minimize these torque and drag problems. Because of fine and very thin film producing capacity of NPs, nano-based fluids can significantly reduce friction factor created between the drilling strings

and the borehole wall as a result of the generation of a continuous and thin lubricated film in the pipe-wall interface. Additionally, fine spherical NPs can form ultra-thin beds of ball bearing type surface between the borehole and the pipe wall which leads to easy sliding of the drill string.

This property shows the importance of the nano-based smart fluid in the reduction of the torque and drag problems in extended reach, horizontal, coiled tubing and multilateral drilling [9].

2.4. Conventional drilling fluids systems

Drilling fluids are roughly divided into three main categories: Oil-based Mud (OBM); Water-based Mud (WBM); and Gas-Based Mud (GBM) [20]. GBM shall not be discussed in this thesis work as they are less commonly used in the industry.

2.4.1. Oil-based muds

Oil is used as a base fluid in OBMs. The mud composition is more complex and more expensive than WBM. Advantages of using OBM are excellent fluid loss control, adequate lubrication to drill bits, no shale swelling, good cutting carrying ability etc. Disadvantages of them are poor bonding between formation and cement as a result of oil wet surfaces, poor filter cake clean up and some possible environmental risks such as seepage into aquifers and inducing pollution etc. [8]. Oil-based drilling fluids are mostly used as a friction reducer compared to water-based mud because, OBM has better lubrication efficiency than WBM [21]. The reason why oil is slippery explained as oil has non-polar property which means that it does not have negative or positive charge. However, water molecules are ionic and naturally charged. Part of water molecules have negative charge and part of them have positive charge. Due to polar property of water, negative and positive charges are attracted to each other based on the Van der Waals forces which leads to the molecules sticking to each other. As outlined, oil is non-polar so, the oil molecules can slide along another very easily compared to that in water molecules [22].

2.4.2. Water-based muds

Water-based drilling fluids consist of brine/water as a base fluid. These muds are environment friendly and disposal of cuttings can be easily done. Linear polymers, cross-linked polymers, bio-polymers, or synthetic polymers are generally used as a viscosifying agent [8].

In Norwegian Continental Shelf (NCS) using WBM in the first top sections is necessary and is usually used as long as wellbore conditions allow. As discussed earlier OBM has better slippery/lubrication efficiency than WBM. This increases interests on addition NPs to the WBM to reduce friction factor between wellbore and drilling string walls. Based on the experimental study done by C. Jahns showed that some nanoparticles especially titania and silica added WBM significantly reduced friction [13]. The main motivation shall be the application of these sort of NPs to OBM and shall be investigating impact of NPs as a friction reducer in OBM.

3. Experimental setup and procedures

Whenever two surfaces are interacted the tribology principles are in action. In some cases friction can be beneficial however, in some cases it is undesirable which can lead to loss of power or wear of the equipment. There are several methods to perform tribology measurements. In this work lubrication effects of nanoparticles contained oil-based mud (OBM) will be measured on the pin-on-disk (POD) apparatus and modular compact rheometer (MCR) modified tribology measuring cell of an Anton Paar apparatus. Furthermore, the rheology behavior of the fluids are measured by applying of the MCR viscometer cell of Anton Paar apparatus. In this chapter, the design of the experiments, methodology and samples used in these experiments will be broadly outlined.

3.1. Pin-on-disk apparatus

In this thesis work, the POD apparatus is adjusted according to the international standardized procedures with the ASTM G99-05 (2010) standard. This standard method provides description of laboratory procedure for measuring the wear of the materials throughout sliding in POD apparatus. Furthermore, obtaining of data, results and graphs are also broadly described in this standard. More information about the experiment setup and procedure shall be explained step by step in the following sub chapters.

3.1.1. Experiment Setup

As mentioned earlier, POD apparatus are used for to determine wear and lubrication characteristics. There are various types of POD apparatuses and all are based on the same standards which are described in the ASTM G99 and DIN 50324 standardization manuals [23]. The good feature of this apparatus is that all kind of liquids can be used as a lubrication in this apparatus. Two specimens, a pin with ball and a disk, are required on the pin-on-disk wear test. The pin is pressed onto a rotating disk under the defined load and is usually set perpendicularly to the disk. Usually, material samples are installed on the disk with the sample holder frame

(Figure 3.1). The pin is usually spherical or cylindrical in shape and its diameter ranges from 2 to 10 mm. whereas, the disk specimen diameter ranges from 30 to 100 mm and its thickness is changing within 2 to 10 mm. Prior to commencement of the test, the rotational diameter is determined depending on the user request. Afterwards, sliding speed and sliding distance is adjusted with respect to the rotational diameter [23].

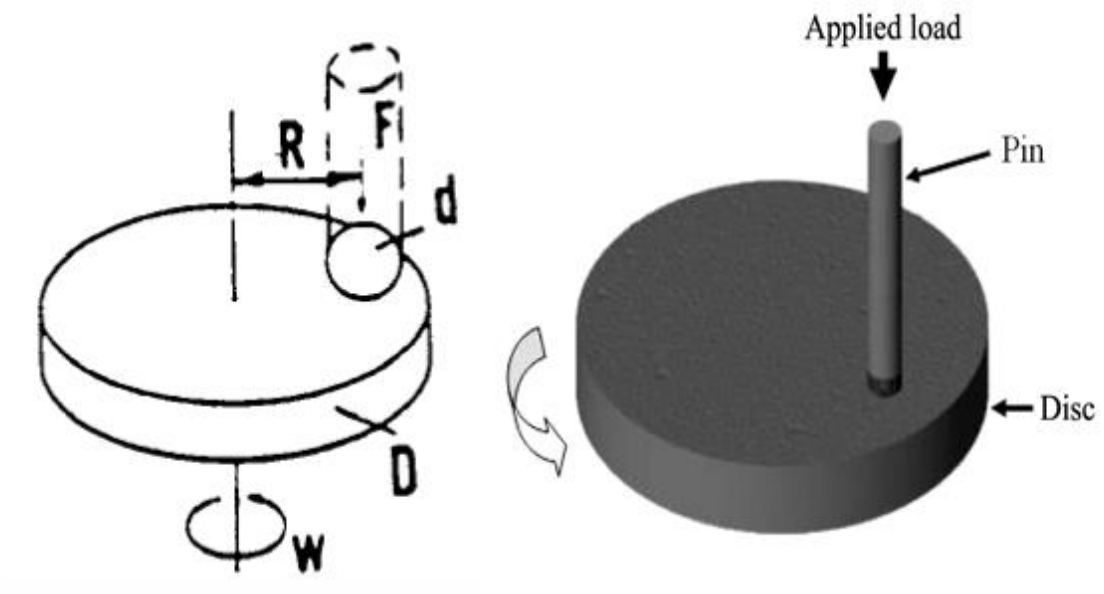

Figure 3.1: Schematic sketch of the POD measuring principle, modified after [23][24].

The following adjustable parameters are the main inputs in the pin-on-disk measurements:

- Load – values of the force in Newtons,
- Speed – sliding speed of the contacting surfaces relative to each other in meters per second,
- Distance - accumulating sliding distance in meters,
- Temperature – temperature of the samples at place near to the wearing contact and
- Atmosphere – the ambient atmosphere such as relative humidity, lubricant, laboratory air, etc. surrounding the wearing contact [23].

Whenever the pin-on-disk measurements start the lost volume is determined by measuring the volume loss of either the disk or the pin. In this case, it is assumed that only one of the specimens is significantly worn, however, another one is unnecessarily affected. According to ASTM G99 and DIN 50324 standardization manuals if the wear volume is only in the pin, the following equations are used to calculate volume loss in mm^3:

$$Vpin.loss = \left(\frac{\pi h}{6}\right)\left(\frac{3d^2}{4} + h^2\right) \quad (3.1)$$

where:

$h = r - (r^2 - d^2/4)^{1/2}$

d = wear scar dimater and

r = pin end redius

It is assumed no significant disk wear.

If the disk has significant volume loss and the pin has negligible abrasion, the following equation is used to calculate volume loss in the disk in mm^3.

$$Vdisk.loss = 2\pi R[r^2 sin^{-1}\left(\frac{d}{2r}\right) - \left(\frac{d}{4}\right)(4r^2 - d^2)^{\frac{1}{2}}] \quad (3.2)$$

where:

R = wear track radius and

r = wear track width

It is assumed no significant wear in the pin [23].

Measuring the accurate radiuses and diameters of the scratches on the material by using the optical 3D confocal microscope and putting them in the equations described above, volume loss can be found [13].

3.1.2. Procedure

As outlined earlier, the pin-on-disk measurements are done based on the ASTM International Standard G99 and DIN 50324. In this experiment phase, POD measurements were conducted in the tribology lab of the Norwegian University of Science and Technology (NTNU) and SINTEF in Trondheim. In Figure 3.2, general view of the POD apparatus is illustrated. Reproducibility of the test and tests in different temperatures are considered advantages of this apparatus.

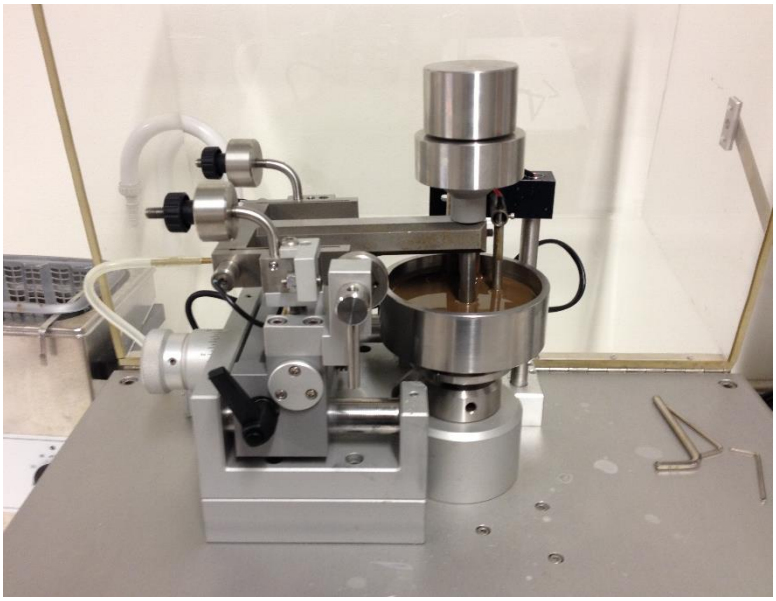

Figure 3.2: Pin-on-disk apparatus with the tested fluid.

Before setting up the experiment, some parts of the pin-on-disk apparatus such as material sample, ball, sample holder with screws etc. need to be cleaned. As illustrated in Figure 3.3, these parts receive an ultrasonic ethanol bath for 6 minutes. This ultrasonic ethanol bath removes unwanted surface contaminations from the material. After having ultrasonic ethanol bath the same materials are washed with the ethanol again and dried with high pressurized air. This is done to make sure that no ethanol content is contained in the material surface before the experiment.

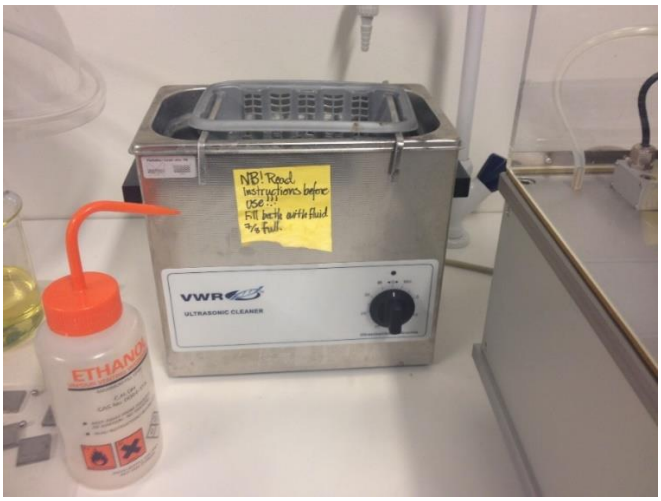

Figure 3.3: Ultrasonic ethanol bath.

After the ultrasonic ethanol bath the material sample is installed. This material sample is a specific casing steel ST 57 and is in 2.5 x 2.5 x 0.5 cm dimensions. It is attached onto the rotating cylindrical disk by the fixation of the sample with the three screws. After fixing of the material sample, ball and pin is prepared. The material of the steel ball used in this apparatus is a stainless steel AISI 316 grade 100. It is in 6 mm diameter. The steel ball is inserted through the cylindrical pin and it is fastened with the screw of the pin on the other end (Figure 3.4).

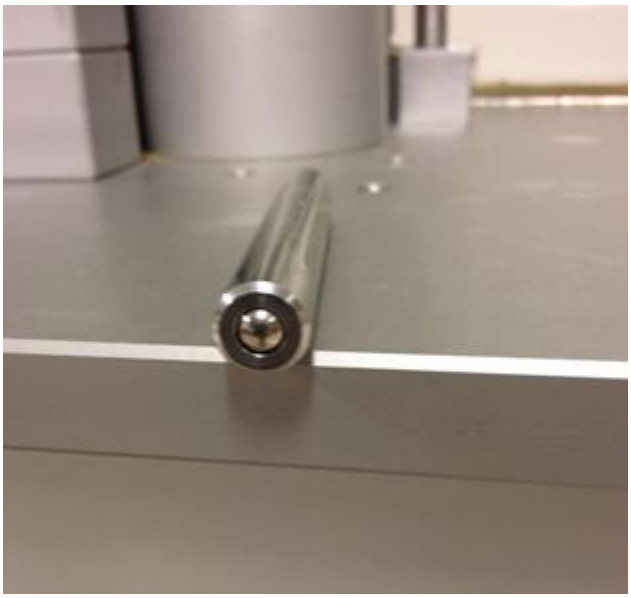

Figure 3.4: The pin with the ball.

The heating spiral is mounted into the sample holder and the disk. In order to make sure that applied load is distributed efficiently to the surface of the material the pin holder is calibrated into the horizontal equilibrium before the experiment starts. In order to check if the arm of the pin holder is horizontally equilibrium, the magnetic level is used (Figure 3.5). Later, it can be left in an inclined position for ease of further preparation.

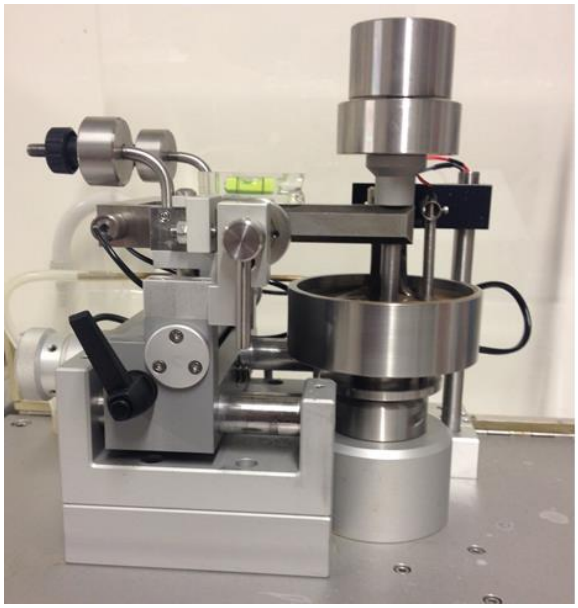

Figure 3.5: Pin-on-disk apparatus gauged with the horizontal magnetic level prior to experiment.

Thereafter, the cylinder basin is filled with the drilling mud. To transfer the increasing temperature through fluid sample, the drilling fluid has to cover heating spiral completely (Figure 3.6).

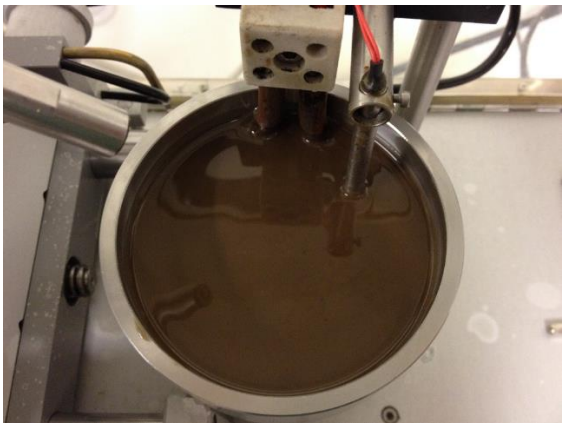

Figure 3.6: Illustration of the heating spiral covered with the tested drilling mud.

Required volume for each test is around 80-100 ml. Moreover, rotational diameter is decided to be set 5 mm for each test with 120 RPM. 10N normal load is used for every experiment. During the POD test series, 50, 75 and 100°C are decided to set. The apparatus is connected to the PC and run with the Tribox 2.10.C programming software (Figure 3.7).

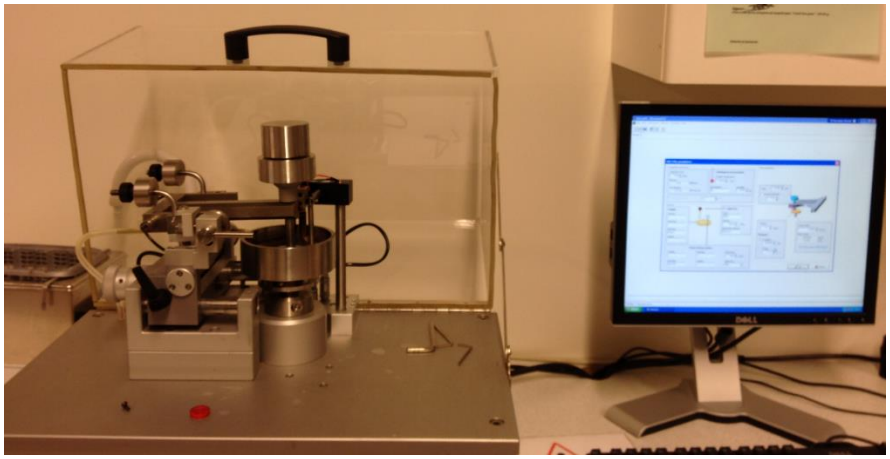

Figure 3.7: Illustration of the pin-on-disk apparatus with the connection to the PC.

The above mentioned parameters as wells as room humidity are set into the software system. Finally, required temperature is put into the software prior to the experiment commencement. Desired temperature can be reach in 15-20 minutes depending on the added temperature value. During the heating up of the fluid sample, the disk is in the stable rotational motion, thus, it helps to distribute temperature constantly through the fluid sample. Since the pin holder is in an inclined position, no friction is recorded before the experiment commences. After the desired temperature is reached the pin arm is lowered and normal force load is added on top of the pin itself. After these steps, experiments are ready to start.

When the experiment is finished the mean value is set automatically in the software system. For further investigations the ball and material sample can be taken for the 3D confocal microscopic observations (Figure B.2). As mentioned earlier, measuring the exact radiuses and diameters of the scratches on the material by the microscope and depending on either the pin or the disk is worn the equation (3.1) and (3.2) are used accordingly to find exact volume loss [13].

3.2. MCR tribology measuring cell

Another apparatus used to measure friction is MCR tribology measurement cell of an Anton Paar. This apparatus allows a static friction test with a concentric steel ball rotates along the three steel plates. This steel plates are fixed to the sample holder and filled with the

experimented fluid. More about the MCR modified tribology measurement cell of an Anton Paar will be outlined in the following subchapters.

3.2.1. Experiment setup

As written earlier, to measure the friction and lubrication properties of the fluid the tribology measuring cell is used. This measurement is based on the ball-on-three-plates principle where the normal force controls the friction force by the rheometer. MCR apparatus is also software-based system as pin-on-disk apparatus. Adjustable inputs are the temperature, the zenith distance of the steel ball, the normal force, bottom of the testing equipment and rotational speed. The given rotational speed of the measurement system defines the sliding speed. The application in this software is arranged based on either Stribeck curve or static friction test where the steady increasing of the torque is maintained [25].

Measuring system shaft for holding the measuring ball, the holder which keep exchangeable plates on a spring system and the temperature system are the main parts of the tribology measuring cell (Figure 3.8). The temperature range varies from -40°C to +200°C. Maximum recorded friction force for the system is 70 N corresponding to the 50 N normal force [25].

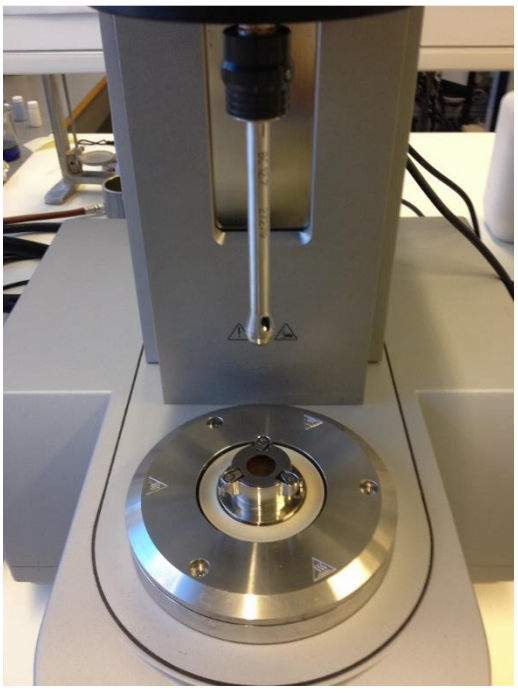

Figure 3.8: The tribological measuring cell with the measurement system.

In this test, friction and lubrication properties of the materials are studied between two surfaces. The friction factor/coefficient (μ) is used to characterize these properties by plotting friction coefficient, μ, versus sliding distance, S_S, or sliding speed, V_S, (Stribeck curve). Firstly, sample holder is screwed to the apparatus and then steel plates are screwed to the sample holder. This will prevent unwanted movements of the steel samples and sample holder during the experiment. Deflection angle (α) and zenith distance (d) together defines the contact points of the steel plates and the measuring ball. Generally, the deflection angle is set starting from 0 mm up to the 5-8 mm depending on the user wish. Figure 3.9 illustrates the schematic drawing of the ball-on-steel plates system and the forces acting at the contact points between inset plates and measuring ball.

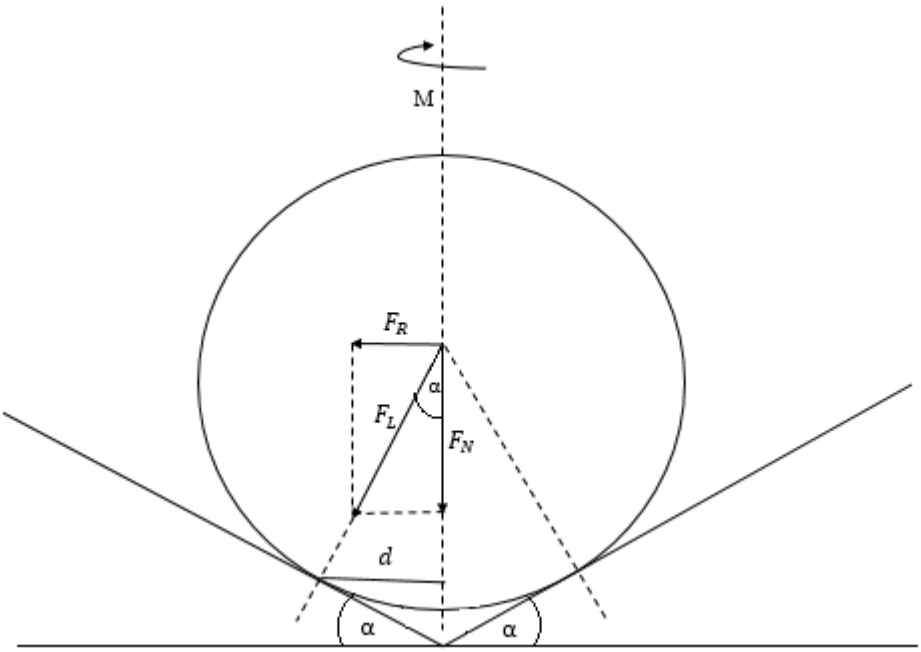

Figure 3.9: Schematic drawing of the tribology measuring cell, modified after [25].

For each test the three steel plates and the measuring ball are changed with the new ones and these new samples are washed and then dried with the pressurized air. Safety gloves and glasses are used to prevent mud from external contaminations and for safety reasons, accordingly.

The experiment is ready when all inputs are added to the software system and the measuring system shaft with the steel ball is lowered and pressed onto the three steel plates with the

predetermined normal force (F_N). To measure friction and lubrication properties of the mud with the MCR tribology measuring cell the following equations are used.

1) Normal load

Normal load (F_L) which is the vertical to the friction surface of the three steel plates and the measuring ball is calculated according to the normal force. Depending on the values of the normal force and the measured deflection angle of the steel plates, normal load is changed.

$$F_L = \frac{F_N}{cos\alpha} \tag{3.3}$$

2) Frictional force

Frictional force (F_R) is dependent on the ball radius and momentum. The momentum is the only parameter effects on the frictional force since the ball radius is constant. The following equation expresses calculation of the frictional force.

$$F_R = \frac{M}{R \cdot sin\alpha} \tag{3.4}$$

3) Friction factor

Friction factor shows lubrication or friction behavior of the sample. When the friction factor is high then lubrication behavior of the sample is low and reversely, when the friction factor is low then lubrication property of the sample is high. It is dimensionless parameter and is defined as a ratio of the friction force to the friction load.

$$\mu = \frac{F_R}{F_L} \tag{3.5}$$

4) Sliding distance and sliding speed

During experiments testing the sliding speed (v_S) and the sliding distance (s_S) are required to illustrate either the Stribeck curve or the static friction test curve. These curves express the friction factor over either the increasing speed ramp with a short measurement point duration or effect of the distance. Sliding speed (v_S) is determined by the rotation of the steel ball with a speed n (Eq. 3.6). The rotation speed is provided by a certain torque (M) which is measured

by the rheometer. Whereas, as expressed in the eq. 3.7 the sliding distance is obtained from the displacement angle (ϕ) and measuring ball radius.

$$v_S = \frac{2\pi}{60} n \cdot r \cdot sin\alpha \tag{3.6}$$

$$s_S = \phi \cdot r \cdot sin\alpha \tag{3.7}$$

3.2.2. Procedure

In this experiment phase, tribology measurements with the MCR were conducted in the laboratory of the Petroleum Engineering and Applied Geoscience Department. In Figure 3.10 a general view of the MCR apparatus with the tribology measuring cell is shown. Repeatability of this test is considered one of its advantages and it is also cheaper to do experiments on this apparatus compare to the pin-on-disk testing equipment. However, there are some drawbacks with this apparatus for instance humidity of ambient environment is not considered during the experiments.

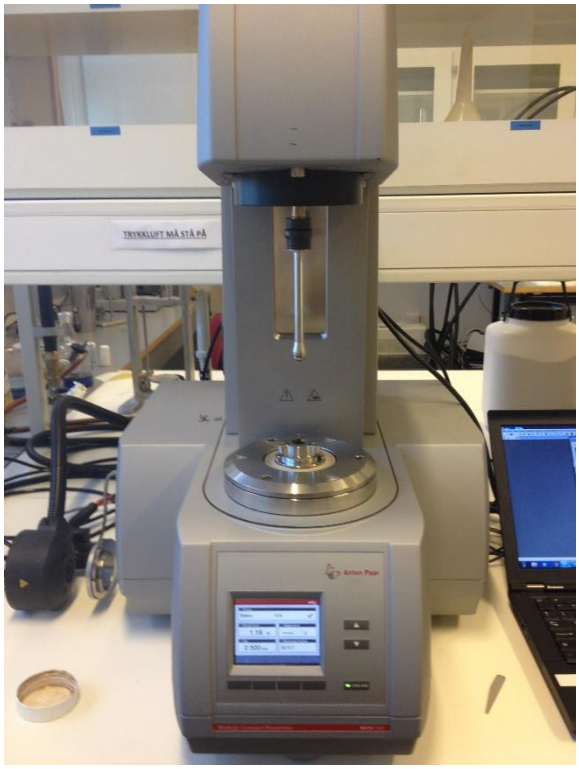

Figure 3.10: MCR rheometer with the tribology measuring cell.

Firstly, main parts of the equipment are properly installed to the MCR rheometer. The tribology measuring cell is aligned to the MCR apparatus and is added to the system automatically by the name of T-PTD 200. All screws are handed tightly to prevent unwanted movement of the samples during the experiment. The cooling system is switched on to the apparatus and connected to the tap water by the hose [25].

The tests are decided to be conducted in 25, 50 and 100°C temperature variations. The volume of the fluid used on each experiment is 2 ml. The steel ball diameter is constant and equal to 12.5 mm. The measuring ball is pushed to the lower end of the measuring system shaft. If the situation allows the steel ball is used at least two times. Since one side of the steel ball is worn during the first test and other side of it can be used for the second test as well.

Then device driver is opened and main parameters and inputs are set to the software system. The gap (zenith distance – d) is set 1 mm and constant for all experiments in this apparatus. When the measuring ball is dig to the fluid samples, the remaining time is counted to start the experiment. Depending on the desired temperature, this time can be between 2-5 minutes range. The material of the measuring ball and plate samples used in this experiments are made up from the steel 316 SS.

The measuring ball and steel plates are washed with the brush and inserted to the Soxhelt equipment to circulate with methanol for an hour. Thereafter, the samples are dried with the pressurized air before each experiment. This helps to remove small scale unwanted particles attached to the surface of the material samples. This equipment is illustrated in the figure 3.11. Additionally, safety glasses, latex gloves and sometimes ear plugs are used for safety and some experimental reasons.

Figure 3.11: Soxhelt equipment.

In this thesis framework, tribology measurements with the MCR apparatus are decided to conduct according to the Stribeck curve, where the speed distribution is increasing as the same for the standard viscometer apparatus. The rotational speeds set in the tests are: 3, 6, 100, 200, 300 and 600 RPM. 100 measurement points are decided to use in the experiments and the tribology measurements for each speed range is 5 minutes which means 30 minutes for each tribology test. Protection lid is used to prevent fluid slipping during the each experiment (Figure 3.12). The calculation of the deflection angle and normal load is automatically done by the rheometer software by using the equation (3.3). Experiment is ready to start when the temperature reaches the desired value.

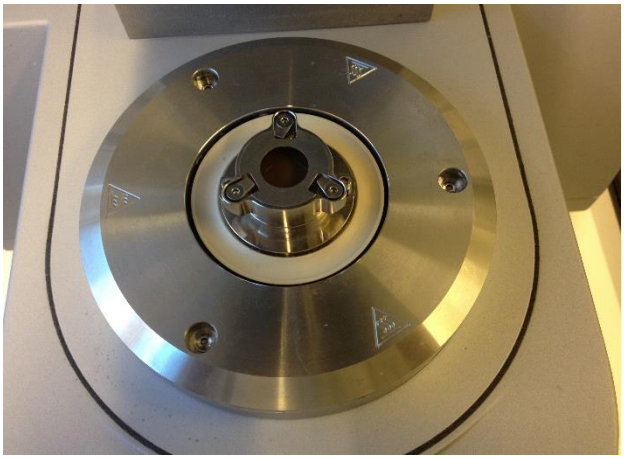

Figure 3.12: Protection lid covers sample holder to prevent spilling of the fluid sample.

Since, the humidity factor is not considered in the MCR tribology test, most experiments shall be done in the same day. All the tests with the MCR will be repeated at least two times to obtain accurate results for the POD experiments.

3.3. MCR viscometer

Generally, in oil fields rheology of the drilling fluids is measured by the model 35 Fann viscometer. However, in this thesis, viscosity measurements are done with the viscometer measuring cell of an Anton Paar under room temperature and pressure. This is one of the advantages of the MCR that measuring viscosity and related parameters is precise, quick and easy. In the following chapters, setup of the experiments as well as the methodology of MCR viscometer will be outlined.

3.3.1. Experiment Setup

MCR viscometer is a mechanical equipment used to measure fluid behavior at varying shear rates. Rotating cylinder called bob and cylindrical cup where the fluid is filled are the main parts of the viscometer (Figure 3.13). The aim of the bob is to generate shear force and this creates a drag force. Depending on the type of the fluids drag force can be different. If the fluid is viscous the drag force will increase and vice versa.

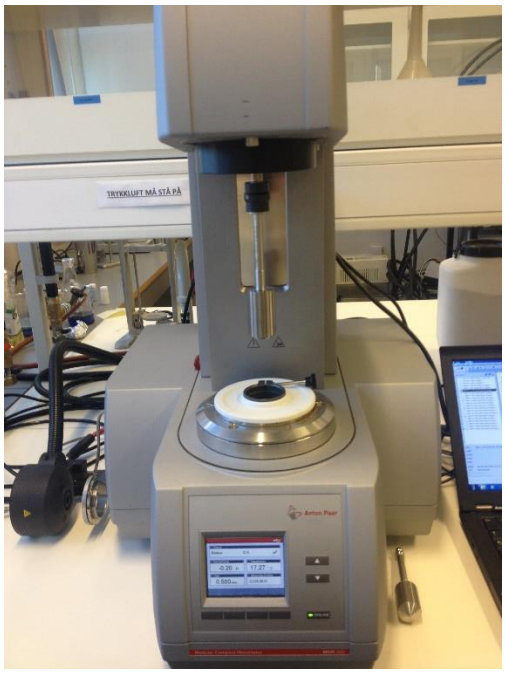

Figure 3.13: General view of the MCR with the viscometer measuring cell.

When the bob starts to rotate in the fluid filled cylindrical cup, share stress and share rate at specific rotational speed is plotted and as a result this flow curve will define the plastic viscosity [26]. During rheology measurements plotted curve is matched one the models illustrated in the Figure 2.4.

In the MCR apparatus, the bob is selected depending on the type of the drilling fluids, WBM or OBM. In Figure 3.14, type of the bob with the cylindrical cup is illustrated for the WBM and OBM in A and B, respectively. In order to prevent wall slipping at high rotational velocities, both types of the bob have axial hollows throughout their surface.

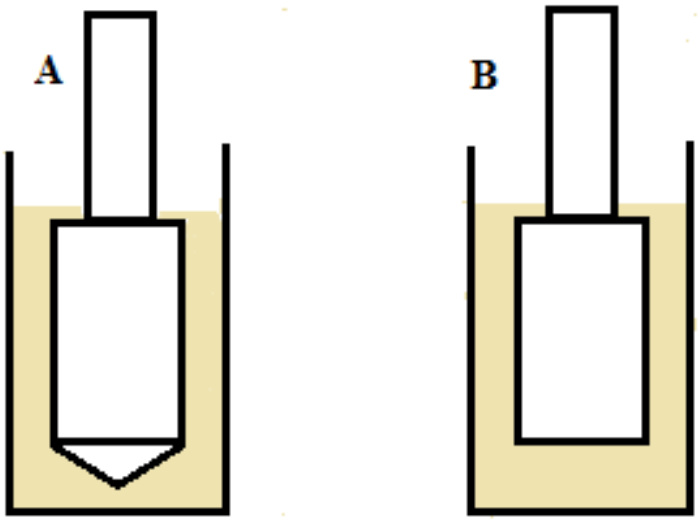

Figure 3.14: A) The cylindrical bob with the cone for the WBM, B) Cylindrical bob for the OBM.

The easiness of MCR viscometer is to measure shear stress and shear rate at specific rotational speed and plot the flow curve automatically by the Rheoplus software. Rotation is provided based on the standard rotational velocities: 3, 6, 100, 200, 300 and 600 RPM. Depending on the type of experiments the rotation speed can be arranged more than 600 RPM.

The shear stress is minimum when the fluid circulation is in the startup phase. Low shear stress occurs in the borehole and pipe walls, whereas, the center of two surface walls refers to the medium shear stress. In the nozzles of the drill bit reflects high shear stress when the fluid passes through them [26]. Since, two concentric cylinder systems i.e. the cylindrical bob is rotated in the fluid filled cylindrical cup (Figure 3.15), the process is similar to the rotation of the drill string in the vertical wellbore.

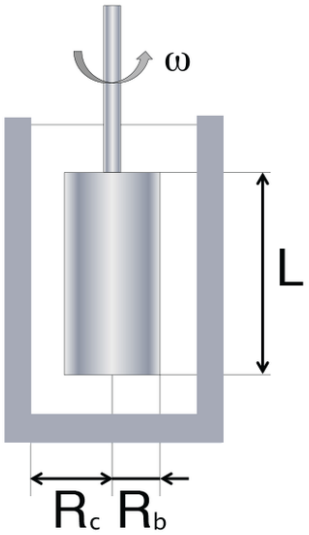

Figure 3.15: The cylinder bob is rotated inside the cup with the given angular velocity [27].

The radius of the gap, the torque and the length of the bob have an effect on the shear stress and shear rate. This influence can be analyzed by understanding the distribution of the stress of the instrumental setup [28]. The shear stress at the bob surface can be calculated from the calculated torque and the geometry (eq.3.8). Whereas, shear rate is measured from the angular velocity and geometry of the system (eq. 3.9). In the equation below variables are the same with those in Figure 3.15.

$$\tau = \frac{M}{2 \cdot \pi \cdot R_b^2 \cdot L} \tag{3.8}$$

$$\gamma = \frac{2 \cdot \omega \cdot R_c^2}{(R_c^2 - R_b^2)} \tag{3.9}$$

where:

$R_c =$ radius of the cylinder cup

$R_c =$ radius of the cylinder bob

$L =$ Length of the bob

$\omega =$ angular velocity

$M =$ measured torque

$\tau =$ shear stre [27].

3.3.2. Procedure

In this thesis, rheology measurements of the fluid sample are conducted by the viscometer measurement cell of MCR of Anton Paar in the laboratory of the Petroleum Engineering and Applied Geoscience Department.

Advantages of the MCR viscometer is equal temperature distribution within the entire cylindrical cup and not any gap leakage occurring at high shear rates. Moreover, drying effect of the sample is negligible. However, having of the air bubbles in the cup during the test, being relatively difficult to be cleaned and slow temperature equilibration is considered disadvantages of the MCR viscometer [29].

Due to the of advantages MCR viscometer mentioned above as well as the higher degree temperature variations capabilities, MCR viscometer measuring cell of the MCR apparatus is more functioned than standard Fann viscometer. For this reason, rheology tests were decided to conduct on the MCR viscometer.

First of all, main parts of the apparatus are correctly set up to the MCR. The viscometer measuring cell is screwed to the MCR apparatus and is set to the system automatically by the Toolmaster™. All required part of the apparatus is screwed tightly to prevent movement during the experiment testing. As tribology measuring cell, the cooling system in the viscometer measuring cell is switched to the apparatus and connected to the tap water.

Since OBM is used in rheology tests, the cylindrical bob for the OBM is selected (see Figure 3.14 B). Whenever, the bob is aligned to the apparatus, it is automatically known by the software of MCR.

The rheology measurements are decided to conduct at the temperatures of 25, 75 and 100°C. The reason is to observe how the nanoparticles affect the rheological behavior of the OBM at different temperatures. Unlike from the WBM, dehydration of the OBM mud is not expected at higher temperatures. Shear thinning behavior of the mud is observed when rotation starts and increases over the time with the applied shear force.

The amount of mud volume required for the concentric cylindrical systems is determined by a marker inside the cylindrical cup. When the measuring head is lowered to measuring position the cylindrical bob must be completely immersed in the sample [29]. The amount of mud

volume required in the viscometer experiments is approximately 10-12 ml per each test. The gap between the calendric bob and bottom of the cup is automatically set to 0.05 mm. The time for the temperature equalization is 3-5 minutes depending on the value of the set temperature for the test (Figure 3.16).

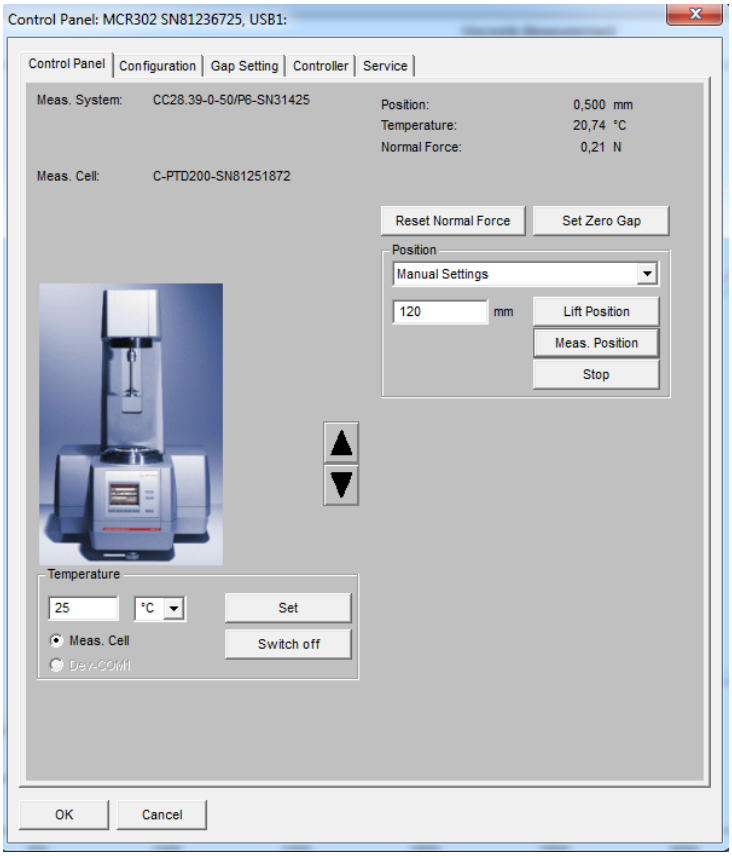

Figure 3.16: Setting of the temperature to the control panel.

Before the experiment starts, all the material samples are washed with the methanol and dried with the pressurized air to remove some scale contamination and the methanol left on the particle surface, respectively. Additionally, all inputs are set before the experiment testing. The temperature and the rotation speed ramp of 3, 6, 100, 200, 300 and 600 RPM are set to the Rheoplus software (Figure 3.17).

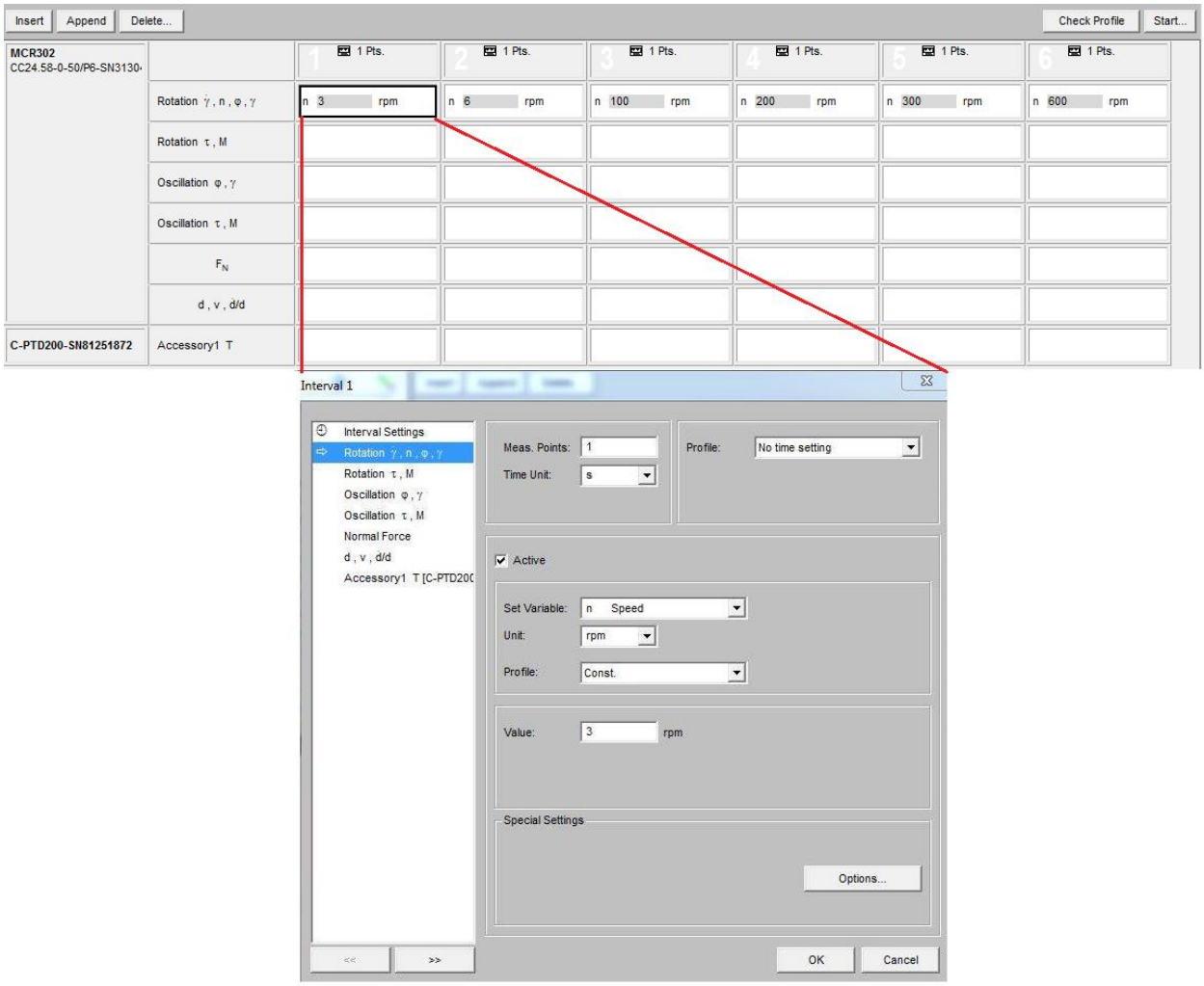

Figure 3. 17. Setting rotational speeds to the Rheoplus software.

More info about the Rheoplus software system and additional parts of apparatus for the viscometer can be found on the MCR Rheoplus manual.

3.4. Chemicals, fluids and sample materials

Nanoparticles are included to the colloidal category based on their particles size [13]. Since, colloidal particles are defined with their influences on the fluid viscosity and the particle interactions, effects of the nanoparticles on the rheological and tribology properties of the drilling fluid will be observed carefully. This means that nanoparticle contained drilling fluids have different behavior compared to the conventional one. For this reason, different temperature variations are applied to the fluid composition. In the following sub chapters,

composition of the fluids and type of the nanoparticles used in the OBM will be outlined broadly.

3.4.1. Composition of the fluid

Since this thesis work is a continuation of the work of C. Jahns [13], the OBM is decided to use in the experiment phase and to compare these results with the results from the WBM used by Jahns.

The oil-based drilling fluid was ordered from the MI-SWICO with the name of "VERSAPRO LS". $CaCl_2$, NaBr, CeCOOH, $CaBr_2$ and KCOOH are the main ingredients used as the internal phase in density. The VERSAPRO LS is an ideal fluid for the drilling through the reservoir in the high temperature drilling environments. Chemical stability, good lubricity, high temperature stability and a low coefficient of friction are considered main features of this fluid. The advantages of using VERSAPRO are the optimizing the rate of penetration (ROP), reduction in torque and drag, stabilizing the wellbore etc. [30].

The density of the drilling fluid was measured by using of mud balance equipment (Figure 3.18). Measuring the density of the fluid with the mud balance method is most reliable and simple. Basically, the measured fluid is filled into a cup and covered with the lid. The lid prevents air bubbles getting trapped in the mud and squeezes excessive mud out of the cup. The measured fluid density is measured by sliding the slider-weight throughout the balance beam. The average density of the measured fluid samples are ranged between 1.20-1.23 g/cm3.

Figure 3.18: Mud balance.

It was decided to add 0.1, 0.25 and 0.5 weight% concentration of different types of nanoparticles to the OBM. The exact mass of each added nanoparticles were measured with the 0.001 error sensitivity scale as illustrated in Figure 3.19.

Figure 3.19: 0.001 error sensitivity scale.

To have correct mass fraction after adding the nanoparticles the total weight of the base fluid with the nanoparticle was taken equal to the 100 g. For example, If 0.25 weight% concentration of nanoparticle is added to the fluid then mass fraction will be 0.25 g for the added nanoparticle and 99.75 g for the base drilling fluid.

3.4.2. Tested nanoparticles

NP contained fluid is a fluid with at least one particle size in the mud in 1-100 nm interval. Generally, NPs can be metals, carbides, metal oxides or fullerenes. In the experimental phase of this thesis, two types of the nanoparticle are used: fumed and compact types of nanoparticles. There are two suppliers of the nanoparticles, Aerosil and Elkem Silicon Company. Fumed silica and titania as NPs, and solid silica were experimented as a microparticle in the fluid sample. In Table 3.1, experimented additives and their properties are mentioned:

Table 3.1: Tested nanoparticles used in the experiment phase.

Name	Average size	Type	Manufacturer
Nano-silica [31][32]	40 nm-100 nm	fumed	Elkem NanoSilica®
Nano-titania [33]	40 nm-60 nm	Hydrophilic fumed	Aerosil®
Micro-silica	30 0nm	Solid	ZEB, NTNU

For comparing the nanoparticles behavior in the fluid micro-silica shall be tested in the POD apparatus. Tribological and lubrication properties of both particles shall be compared with each other and importance of the nanoparticle contained mud will be investigated.

4. Experimental results

Objective of the experimental phase was to conduct tribology and rheology measurements on the OBM with and without nanoparticles. Tribological measurements were performed on the tribology measuring cell of MCR and the POD apparatus, whereas, the rheological tests were done with the viscometer measuring cell of MCR. Since the experiments on the MCR are cheaper than those on the pin-on-disk apparatus, tribological properties were measured with the MCR prior to the POD test. The main reason to prioritize the MCR was to decide further plan for POD apparatus. In this chapter, final results from the experimental procedures will be outlined. The whole data is summarized and presented in the appendices.

4.1. MCR tribology measurement results

Silica and titania were the tested nanoparticles with 0.1, 0.25 and 0.5 weight% concentrations in this apparatus. All the experiments were tested for 25, 50 and 100°C. Each test repeated two times in different periods to obtain accurate results, which took 30 minutes at the six speed intervals and with 100 measurements points. Since friction factor is generated for each point, mean value is taken for each speed range and also for the total test to evaluate the tribology properties. Complete measured friction factors and the other data are summarized and tabulated in Appendix A.

Figure 4.1 and Figure 4.2, visualize the obtained friction factors when silica and titania nanoparticles are added in OBM. According to Table A.4 and A.6 in Appendix A and the presented graphs below, the highest friction factor of 0.283 was generated with 0.5 weight% silica- based mud. Whereas, the minimum friction factor of 0.201 was recorded for the 0.25 weight% titania-based mud. Additionally, other friction factors also mentioned on these graphs, where 0.1, 0.25 and 0.5 weight% of added nanoparticles were colored red, green and black. The reference friction factors were mentioned with the blue color.

Mean friction factor for silica particles with 0.1 weight% at 50°C, 0.25 weight% at 50°C and 100°C, and 0.5 weight% at 50°C showed reduction in friction compared to those in reference

OBM. The rest of the average values of friction factor for silica particles showed increase or similar values of friction factor compared to the reference OBM with the same parameters.

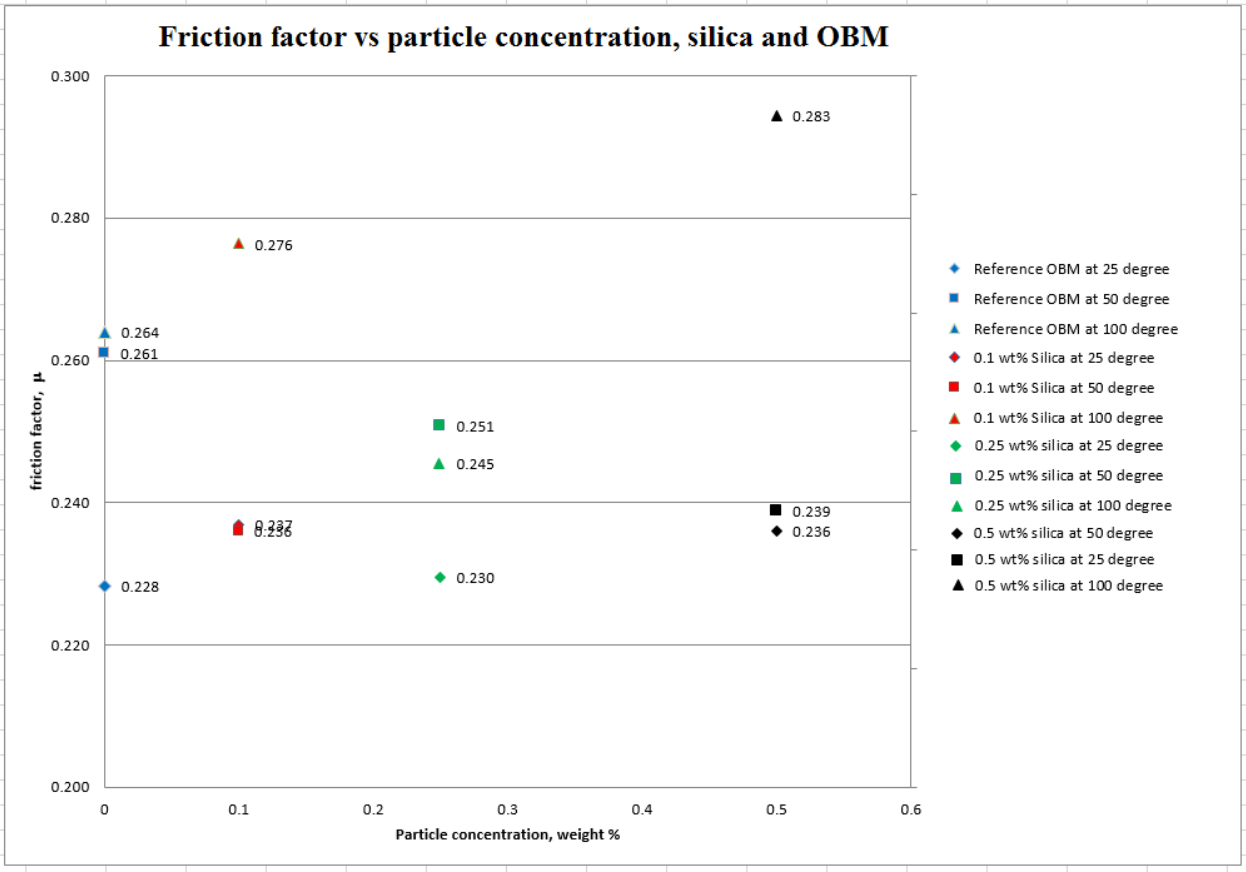

Figure 4.1: Friction factor of silica added fluids and reference OBM vs particle concentration.

On the other hand, average friction factor for titania particles with 0.1 weight% at 100°C, 0.25 weight% and 0.5 weight% at all applied temperatures in this experiment recorded reduction in friction compared to those in reference OBM. While, almost equal values of friction factor were obtained with 0.1 weight% silica particles contained OBM at 25°C and 50°C in comparison to the values of reference OBM.

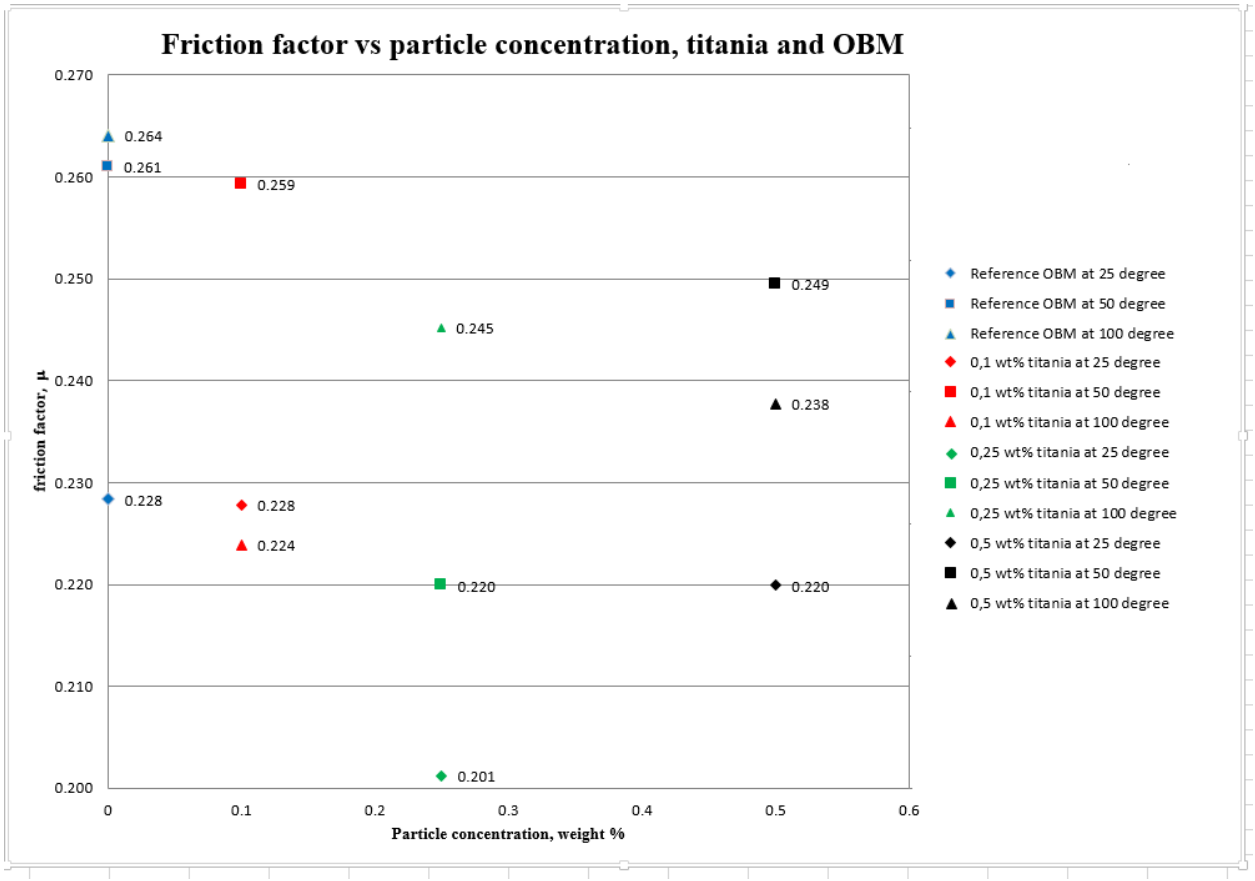

Figure 4.2: Friction factor of titania added fluids and reference OBM vs particle concentration.

To find the relationship between temperature and friction coefficient, 0.1, 0.25 and 0.5 weight% tested fluids were examined at 25, 50 and 100°C. The results for the silica, titania and reference OBM were summarized in Table A.1-A.6, see appendix A. Friction factor for silica and titania added fluids is illustrated compared with the reference OBM in terms of the particles size and temperature in Figures 4.3 and 4.4.The concentration of 0.1, 0.25 and 0.5 weight% nanoparticles were colored with red, green and black, respectively. The reference mud is always shown with the blue color.

In Figure 4.3, the relationship between friction factor and temperature is shown for the silica nanoparticles contained OBM. No friction reduction was recorded for any weight% of nanoparticles at 25 °C. For 0.1 and 0.5 weight% added nanoparticles friction coefficient is increased at 100°C. Interestingly, 0.25 weight% of silica nanoparticles showed reduction in friction at the temperatures of 50 and 100°C. More details of the results can be found in Table A.2-A.4 presented in Appendix A.

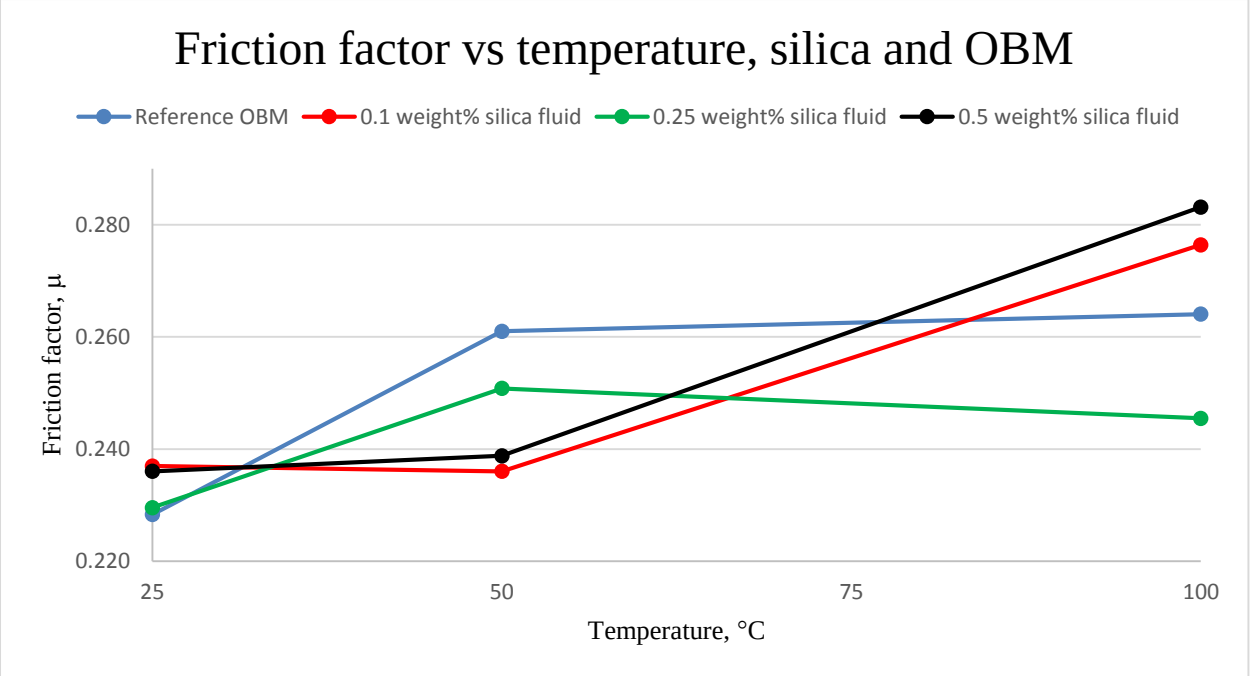

Figure 4.3: Relationship between friction factor and temperature with silica-based mud.

In Figure 4.4, the same relationship between friction factor and temperature is illustrated for the titania-based muds. At 25°C and 50°C temperatures, 0.1 weight% titania added fluid showed almost the same friction factor compared to the reference OBM. The remaining tests with the titania added fluids showed reduced friction for all cases (Table A.5-A.7).

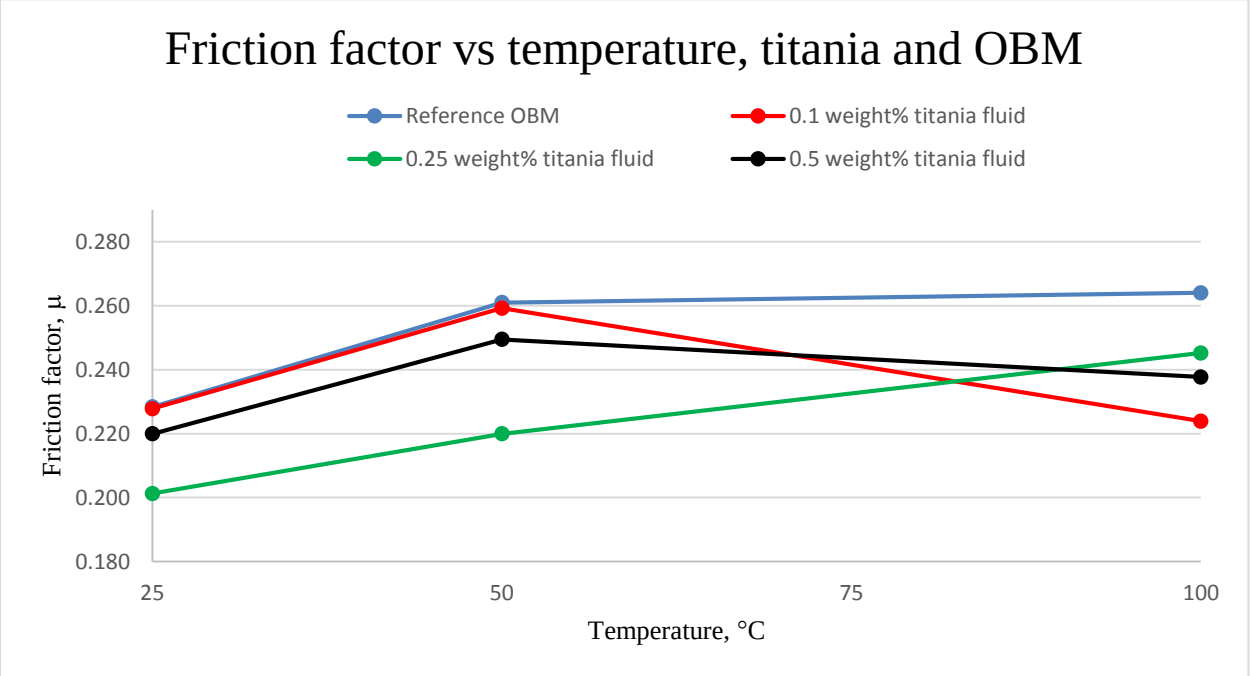

Figure 4.4: Relationship between friction factor and temperature with titania-based mud.

Figures 4.5 and 4.6 show the friction factor of silica and titania added fluids against sliding speed interval. Since the good results in friction reduction were achieved at 50°C for the both silica and titania added fluid, the relationship between the friction and sliding speed is presented at 50°C. Additionally, values of friction coefficient from the MCR are not reliable, meaning that the graphs can be different in reality. Information about variation of friction factor versus sliding speed with respect to the temperature for other concentration of silica and titania added fluids can be found in Appendix A, see Figure A.1-A.4.

For easy comparison, silica added fluids and reference OBM are shown in the same graph. Increasing friction factor were recorded for 0.1 and 0.25 weight% silica added fluids from 3 to 200 RPM, whereas, in 0.5 weight% of silica added fluids the friction factor was slightly decreased from 3 to 6 RPM then showed an increasing trend from 6 to 200 RPM. Friction factor variations after 200 RPM were not stable. However, except for 0.1 weight% of added silica fluids, all other silica fluids showed less friction at 600 RPM compared to that at 3 RPM.

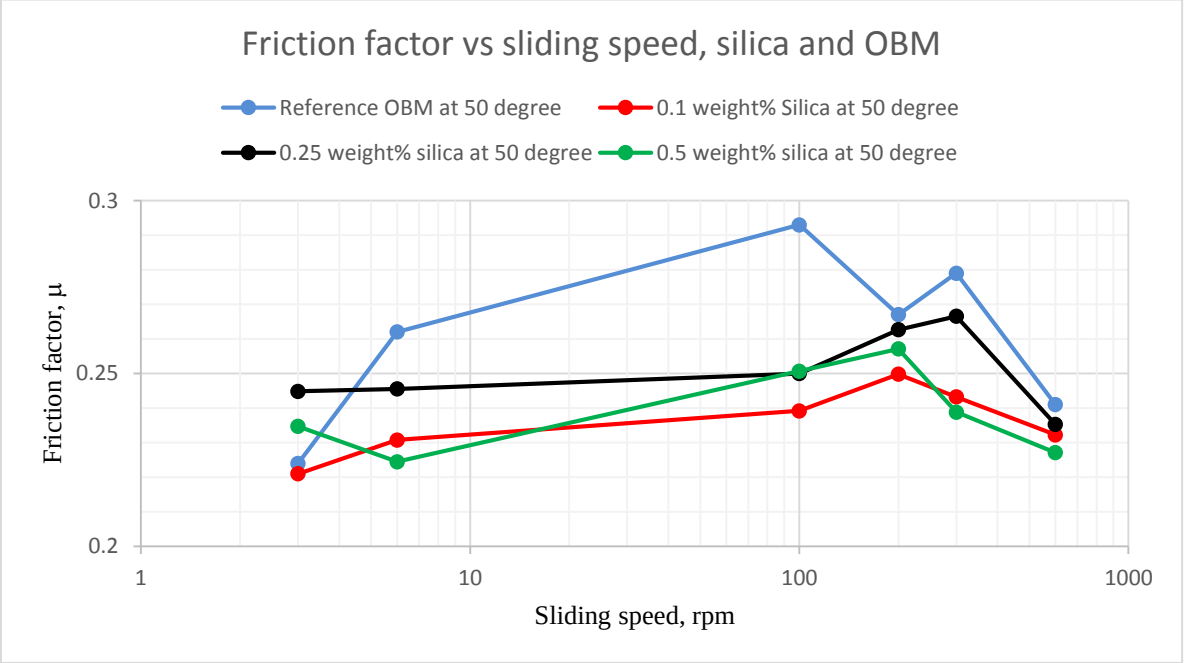

Figure 4.5: Dependence of friction factor on the sliding speed with the silica-based mud at 50°C.

Similar trend were achieved for the titania added fluids as that for silica added fluids. Surprisingly, 0.1 weight% of titania started with the high friction factor at 3 RPM and the friction factor slightly decreased from 3 to 600 RPM.

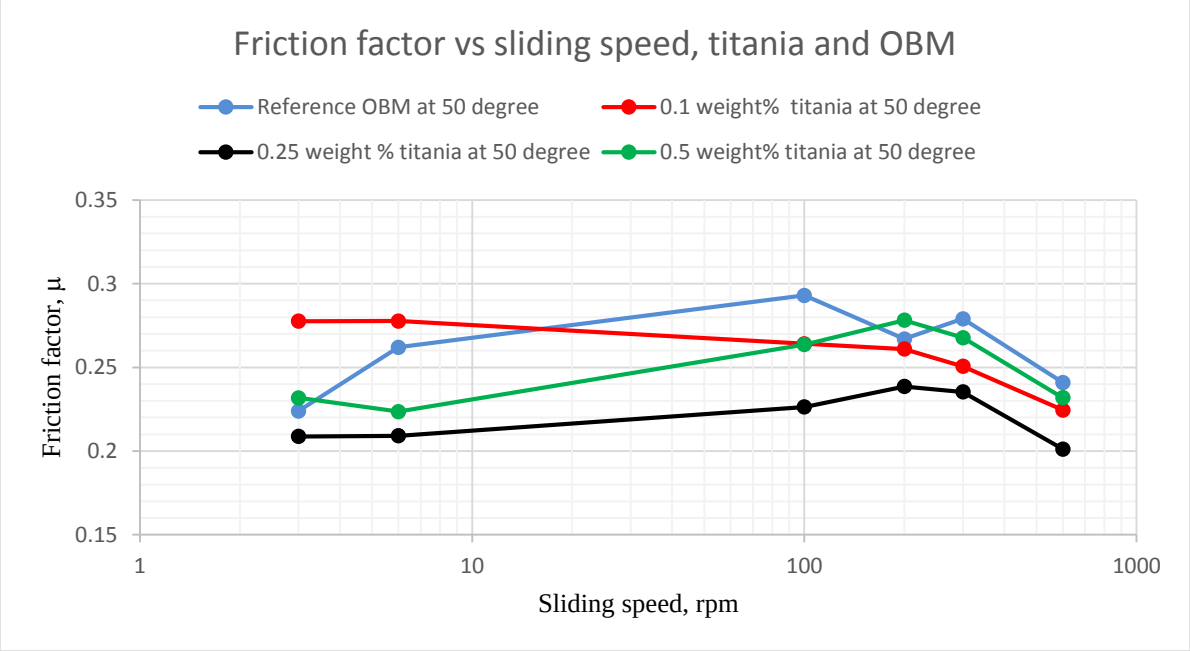

Figure 4.6: Dependence of friction factor on the sliding speed with the titania-based mud 50°C.

4.2. Pin-on-disk Tribology Measurement Results

Since experiments with the POD testing equipment is expensive, firstly, tribology measurements were performed with the MCR. Then, new plan were prepared for the tribology test with the POD apparatus. 0.25 and 0.5 weight% concentrations of silica and titania added fluids were decided to be performed at 50 and 100°C. Additionally, the tribological properties of the micro-silica particles-based mud was also measured with the pin-on-disk apparatus to compare the importance of nanoparticles over micro-scale particles. However, in the first two tests at 100°C, the testing fluid dehydrated and lost its ability with being more viscous than expected, see Appendix B (Figure B.1). Therefore, all experiments were decided to be performed at the temperatures of 50 and 75°C.

As described in the procedure subsection, a set of input data were introduced to the program to make the analysis of the friction factor existing between the steel plate and the ball. The experiments were run for both the reference OBM and NP added fluids. To be able to make the best of the comparison of the results, the highest value of the measured value of the friction factors for the specified fluid were chosen to be compared to the lowest value of that for the reference OBM. For the further details, the reader is referred to the discussion section.

Mean values of the friction factors shown in the graphs are tabulated in Table B.1. Since reproducibility and reliability are the main advantages of using POD apparatus, at least two experiments were performed with the same tested fluid. Figure 4.7 illustrates the reference OBM that tested two times at the temperature of 50°C and the graph which has the lowest value was taken for further comparison with NPs added fluids.

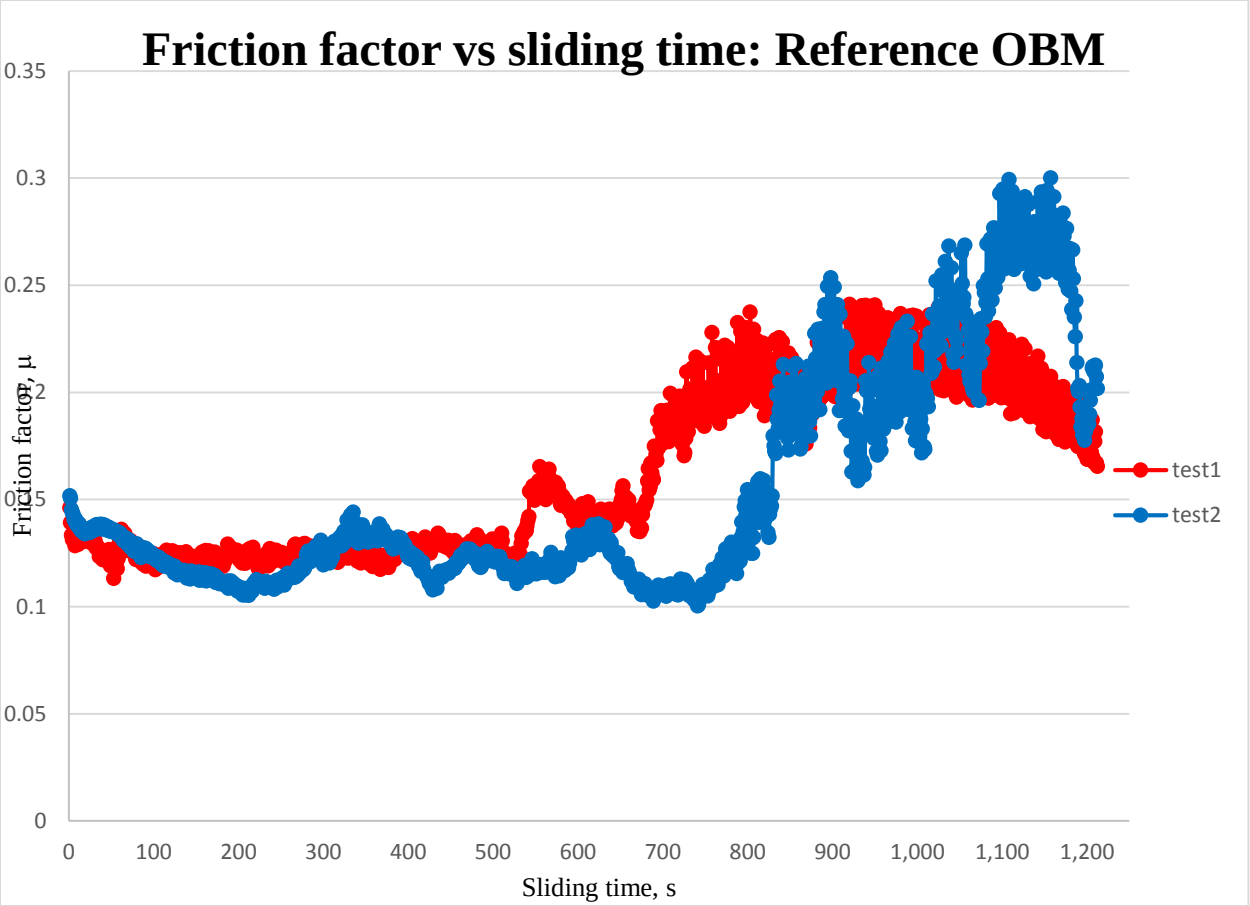

Figure 4.7: Friction factor of reference OBM at 50°C**.**

In some cases, the first two tests showed larger deviations from each other, therefore, the third test was conducted. As an example, 0.25 weight% silica added fluids at 50°C can be mentioned for this specific case. The results from Test 3 confirmed the invalidity of Test 2. Consequently, for the matter of the accuracy, the results of Test 3 were chosen for the next step of the analyses (Figure 4.8).

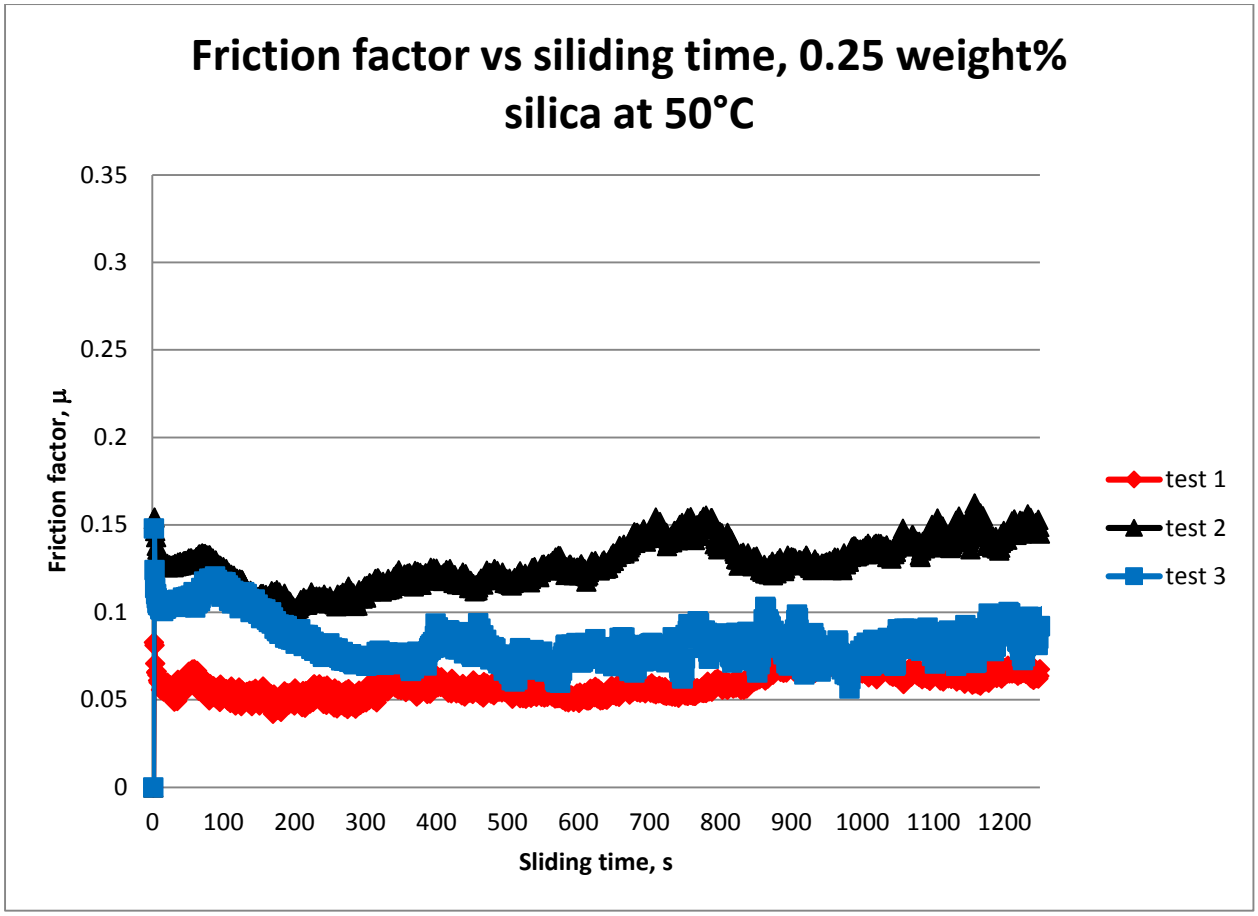

Figure 4.8: Friction factor of 0.25 weight% of silica-based mud at 50°C.

In Figure 4.9, the friction factor of reference OBM was compared to 0.1 weight% and 0.25 weight% of silica added fluids at a temperature of 50°C. According to the results, 0.1 and 0.25 weight% of silica contained OBM showed 17% and 47% reduction in the friction. Where the mean friction factor reduced from 0.1571 to 0.1305 and from 0.1571 to 0.0828 for 0.1 and 0.25 weight% of silica-based mud respectively.

However, no friction reduction was recorded for the same concentration of silica added fluids at the temperature of 75°C, see Figure 4.10.

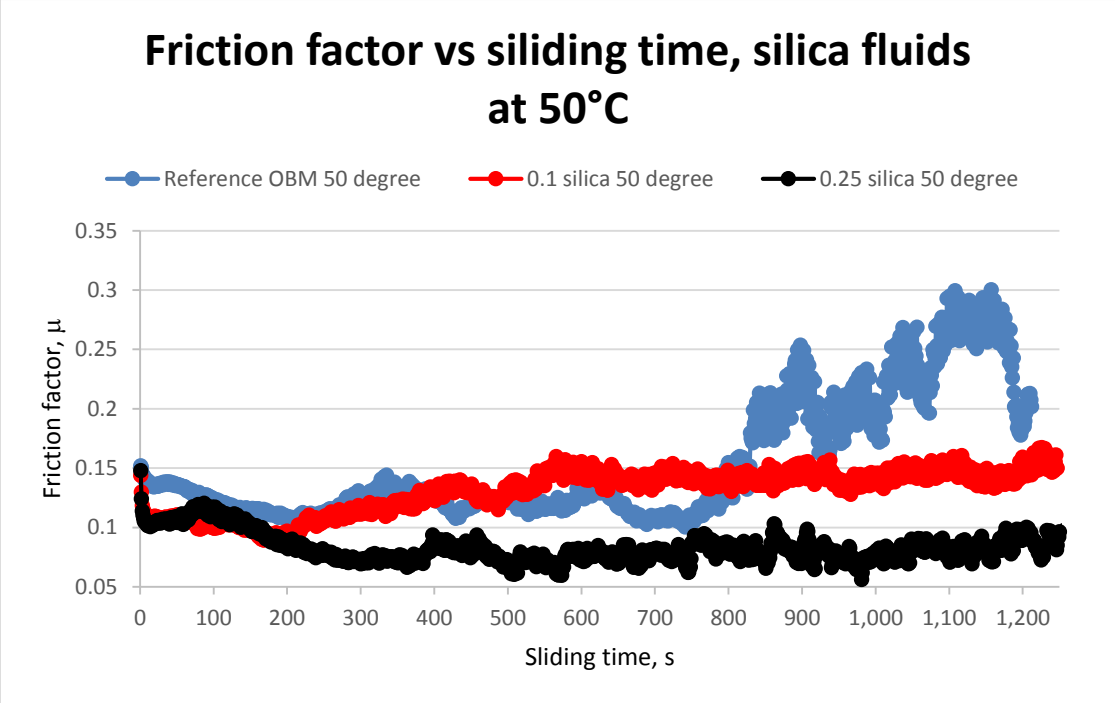

Figure 4.9: Friction factor of silica-based mud at 50°C.

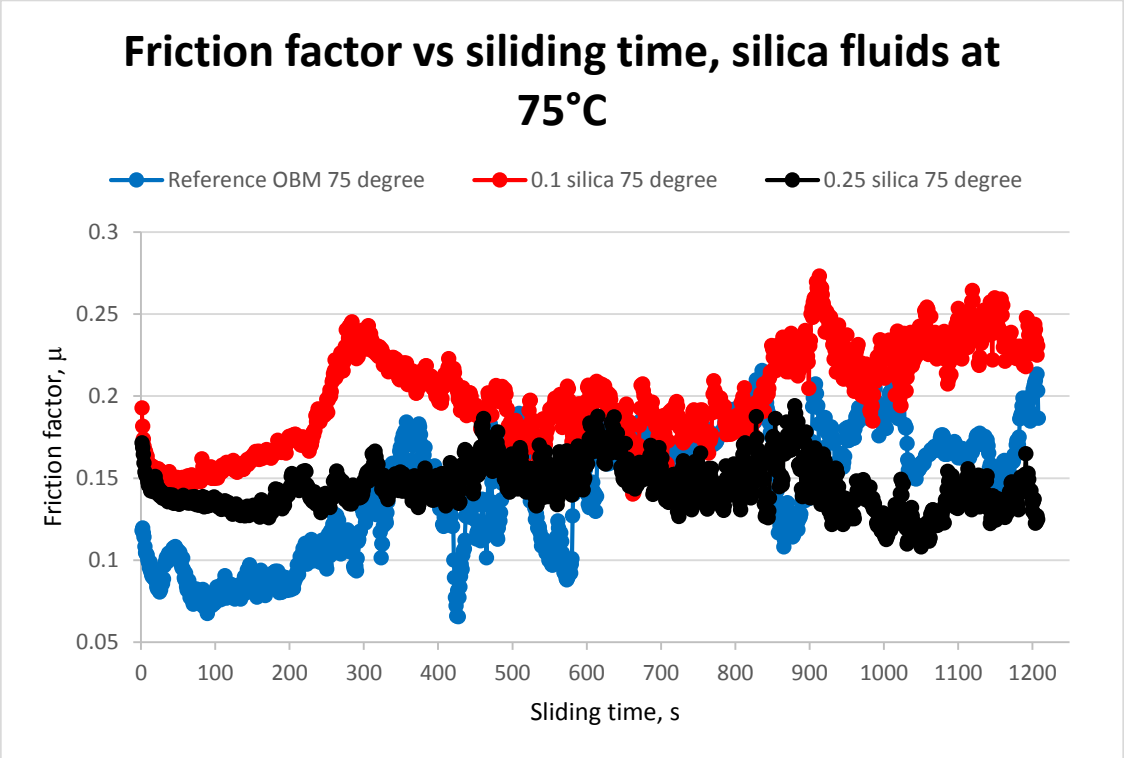

Figure 4.10: Friction factor of silica-based mud at 75°C.

The friction factor of titania-based muds with different concentrations are illustrated in Figure 4.11 and 4.12. Again, reduced mean value of friction was achieved with the 0.1 and 0.25

weight% of titania at the temperature of 50°C. The mean friction factor with 0.1 and 0.25 weight% of titania added fluids were reduced by 14% and 26%, respectively.

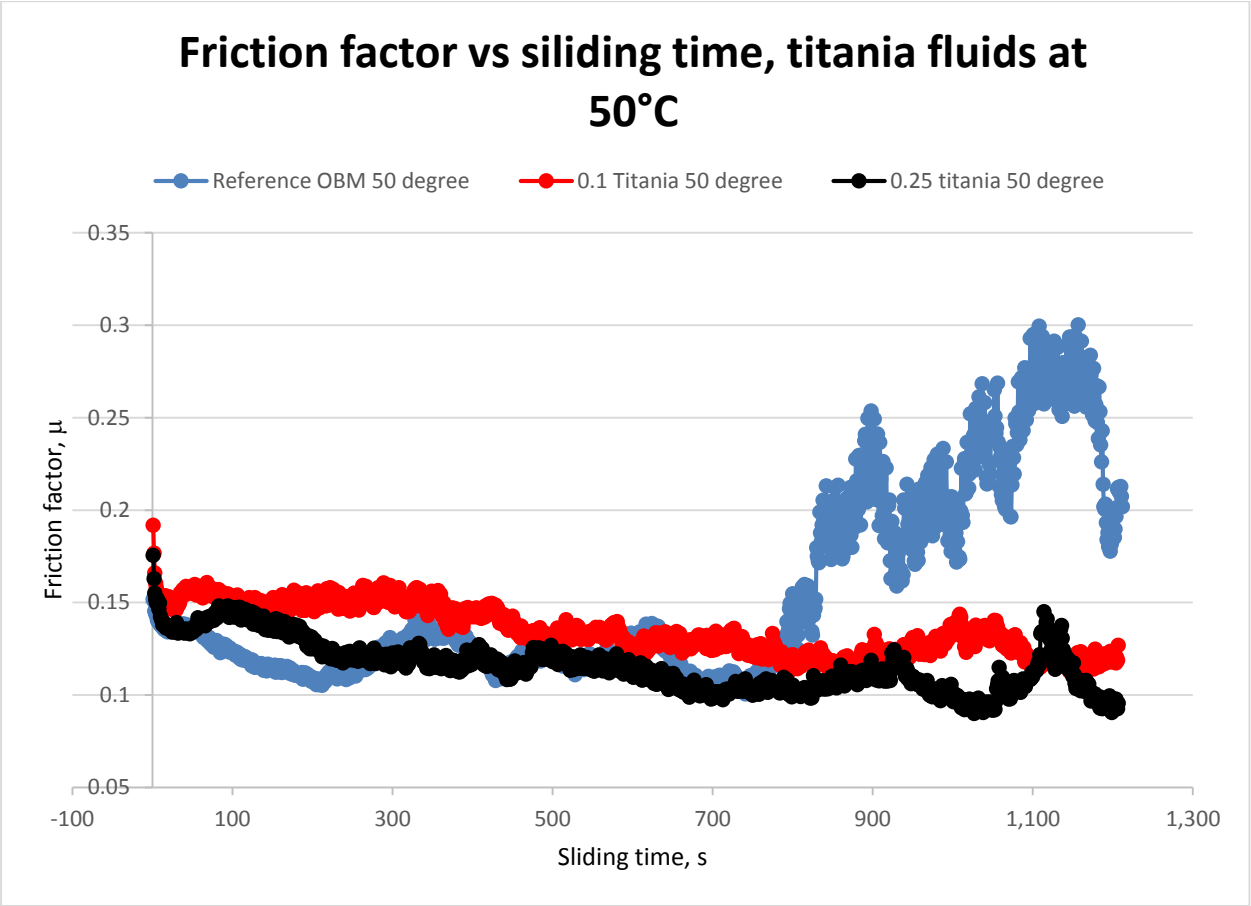

Figure 4.11: Friction factor of titania-based mud at 50°C.

Unlike silica added fluids, 0.1 and 0.25 weight% of titania added fluids at 75°C showed reduction in friction. 0.1 and 0.25 weight% added titania NPs reduced friction from 0.157 to 0.135 and from 0.157 to 0.115, accordingly (Figure 4.12).

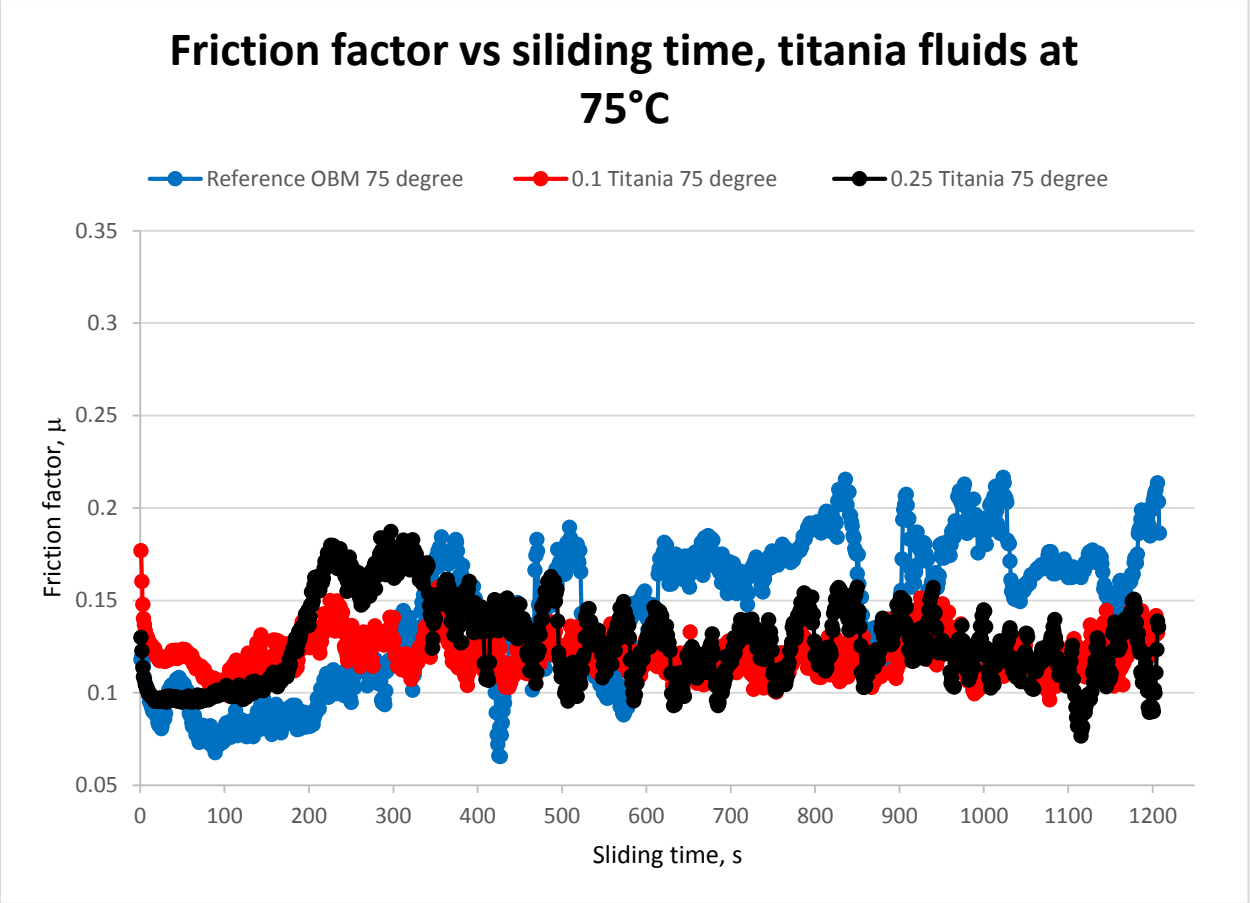

Figure 4.12: Friction factor of titania-based mud at 75°C.

To show the preference of NPs added fluids over the microparticles ones, 0.1 and 0.25 weight% micro-silica was added to the reference mud and tested at 50°C and 75°C. As shown in Figure 4.13 and 4.14, mean friction factors were reduced by 16% and 14% for the 0.1 and 0.25 weight% of micro-silica added fluids at 50°C. However, 0.25 weight% of added micro-silica showed 50% increase value of mean friction factor.

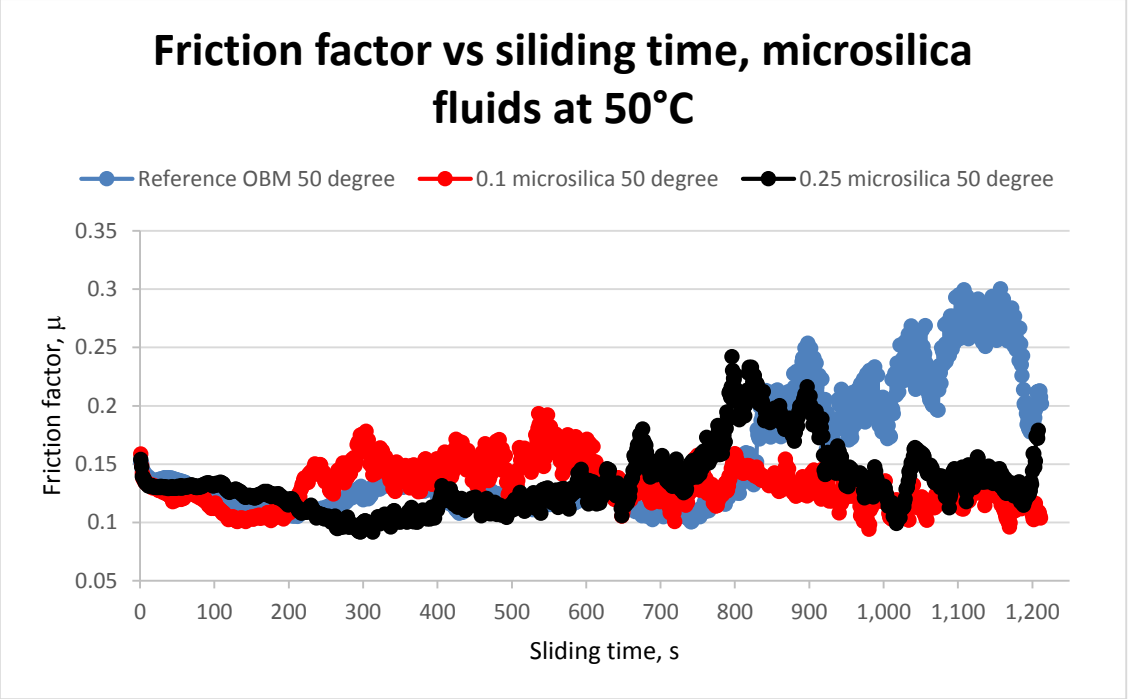

Figure 4.13: Friction factor of microsilica-based mud at 50°C.

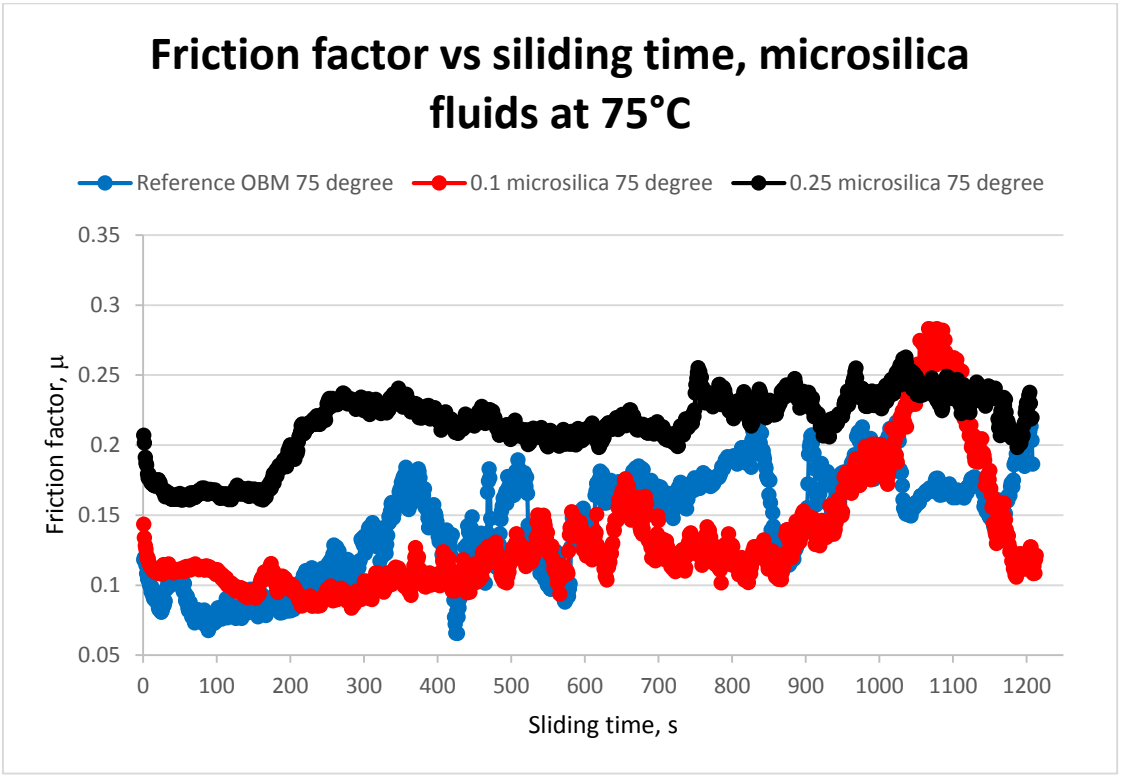

Figure 4.14: Friction factor of microsilica-based muds at 75°C.

Moreover, optical 3D confocal microscopic analyses were also performed on the tested disk samples to extract some parameters for loss volume calculations in the disk. The results of

these measurements are included in Appendix B. Although six disk samples were analyzed with the confocal microscope, no scar depth could be measured by the microscope. The reason are the low values of mean friction factor in all cases and the thin scratches resulted from the ball. For example, Figure 4.15 and 4.16 are illustrated the 3D view of the tested sample with the reference OBM at 50°C and sample itself is shown in Figure B.3. The scar depth is determined by the distance between vertical green and red lines provided by the profile diagram According to the diagram shown in Figure 4.16, the scar depth is equal to zero. Therefore, no volume calculations were performed. This case is the same for all the samples analyzed by optical 3D confocal microscope. Some images taken from these analyses are given in Appendix B.

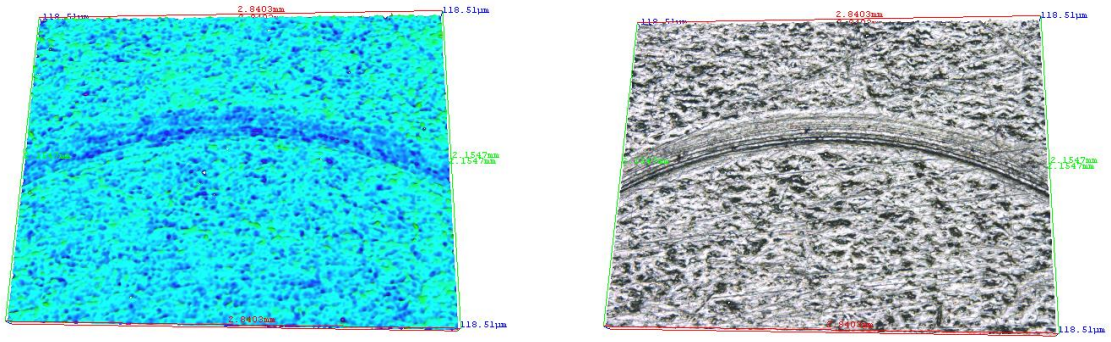

Figure 4.15: İmage of disk sample scratch created with reference OBM at 50°C.

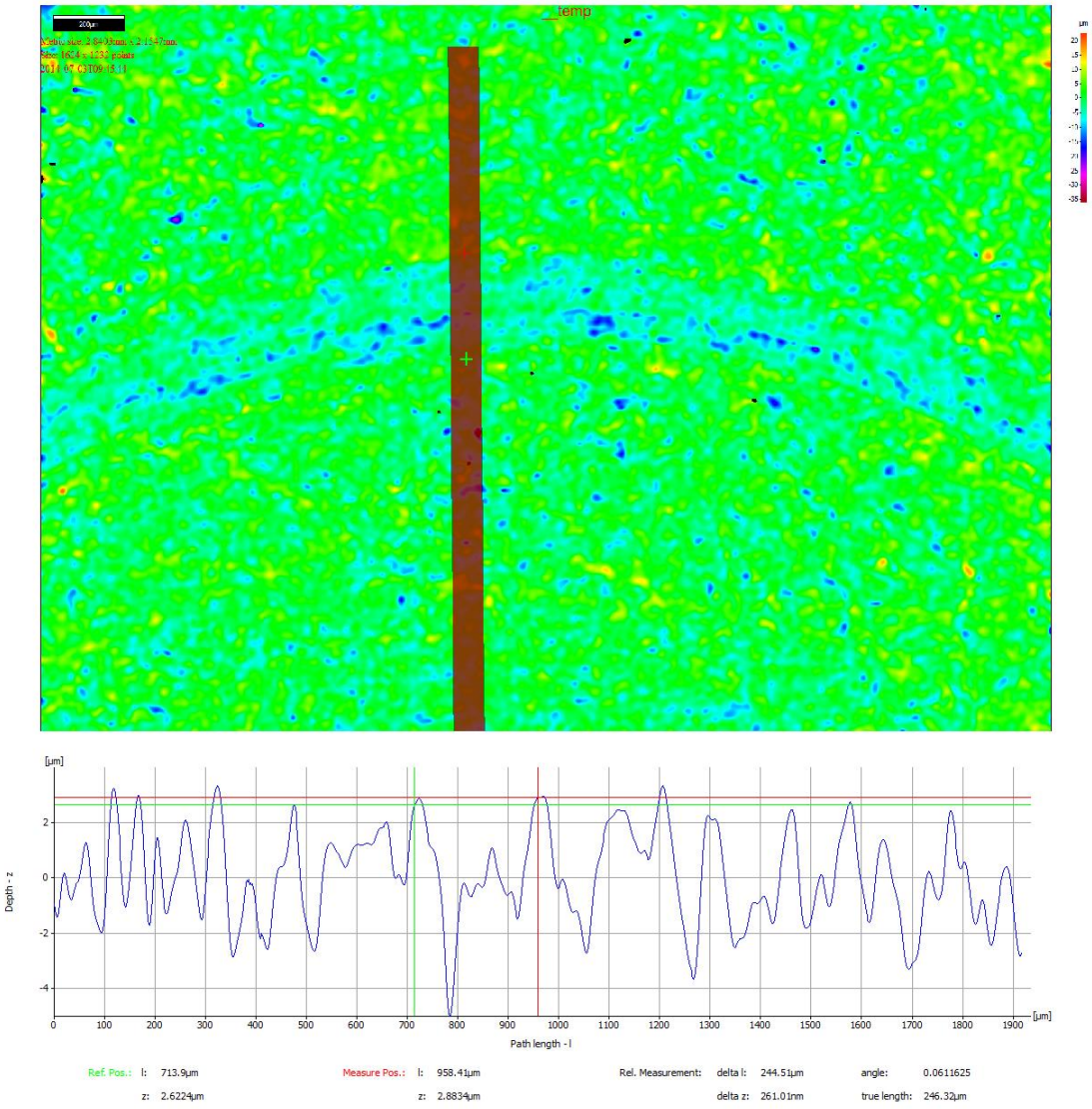

Figure 4.16: Profile diagram of the scratched sample with the reference OBM at 50°C.

4.3. MCR viscometer measurements

After adding the NPs, the rheological behavior of the drilling fluids can go through some changes. Therefore, rheological measurements were tested in some specific concentration. These investigations were performed by the MCR viscometer based on the procedure explained in the previous chapter.

The tested mud with the 0.1, 0.25 and 0.5 weight% of silica and titania added NPs were investigated at the temperatures of 25, 50 and 100°C. The main parameters from this experiment were tabulated in the Appendix C.

Drilling fluids both with and without NPs followed Herschel-Bulkley model and showed close curves relative to each other. Since good results were obtained for reduced friction using 0.25 weight% of silica and titania contained mud at a temperature of 50°C, rheological graphs mainly describe these fluids. However, combination of other concentration at different temperature is also mentioned in this section.

The rheological behavior of the reference OBM at different temperatures is shown in Figure 4.17. The yield stress is almost the same and close to the zero at different temperatures. As seen from the figure, increasing temperature results in decreased shear stress and plastic viscosity. Thus, in some points, the fluid can be even considered as Newtonian fluid.

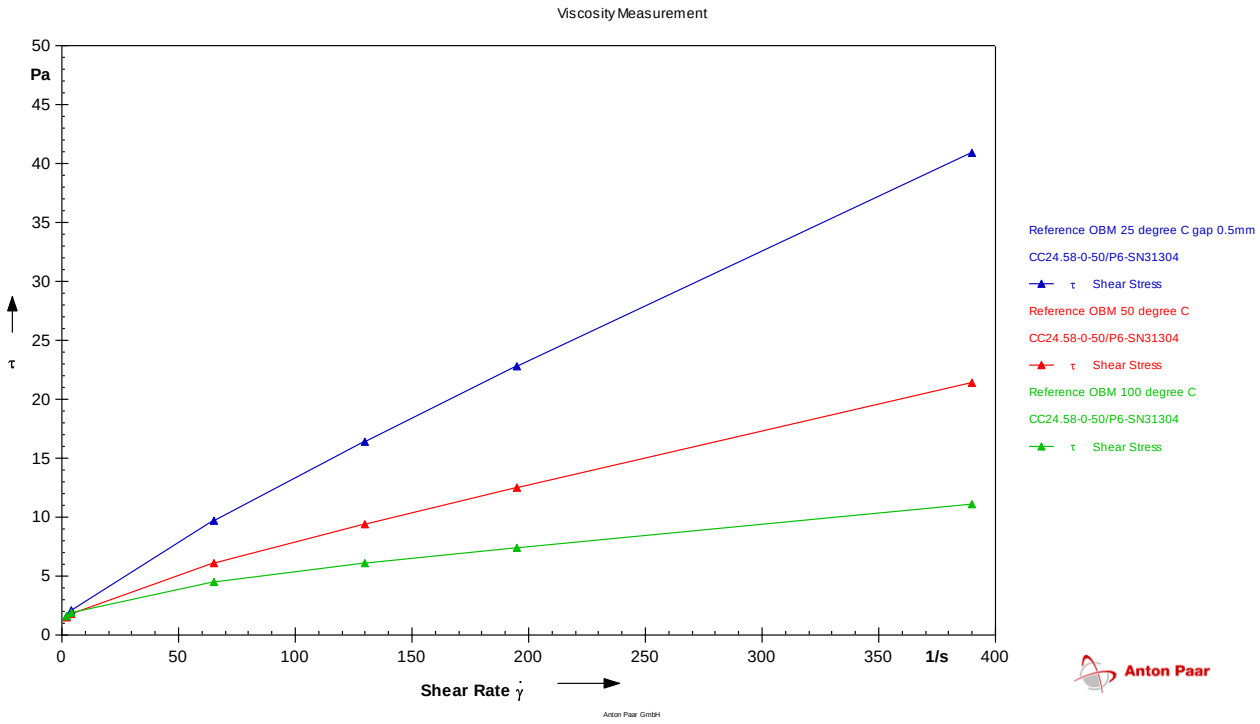

Figure 4.17: Rheological measurements of reference OBM.

0.25 weight% of silica and titania added fluids were also investigated at 25, 50 and 100°C. The curves in Figure 4.18 and 4.19 show the same trends as described for the reference OBM.

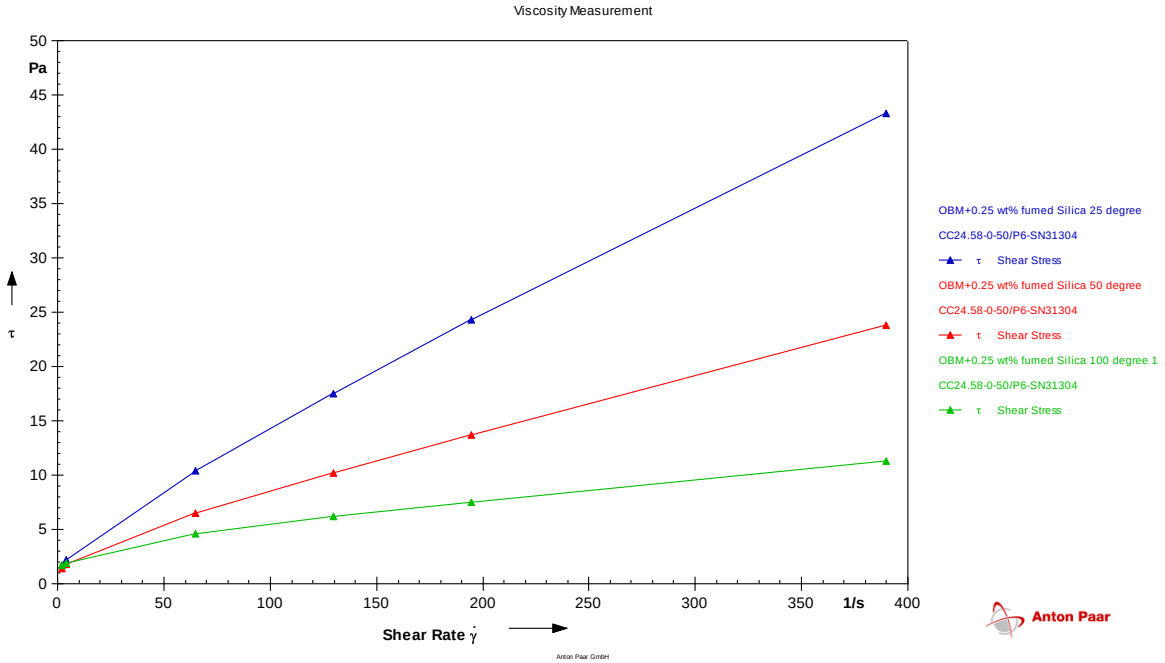

Figure 4.18: Rheological measurements of silica-based mud.

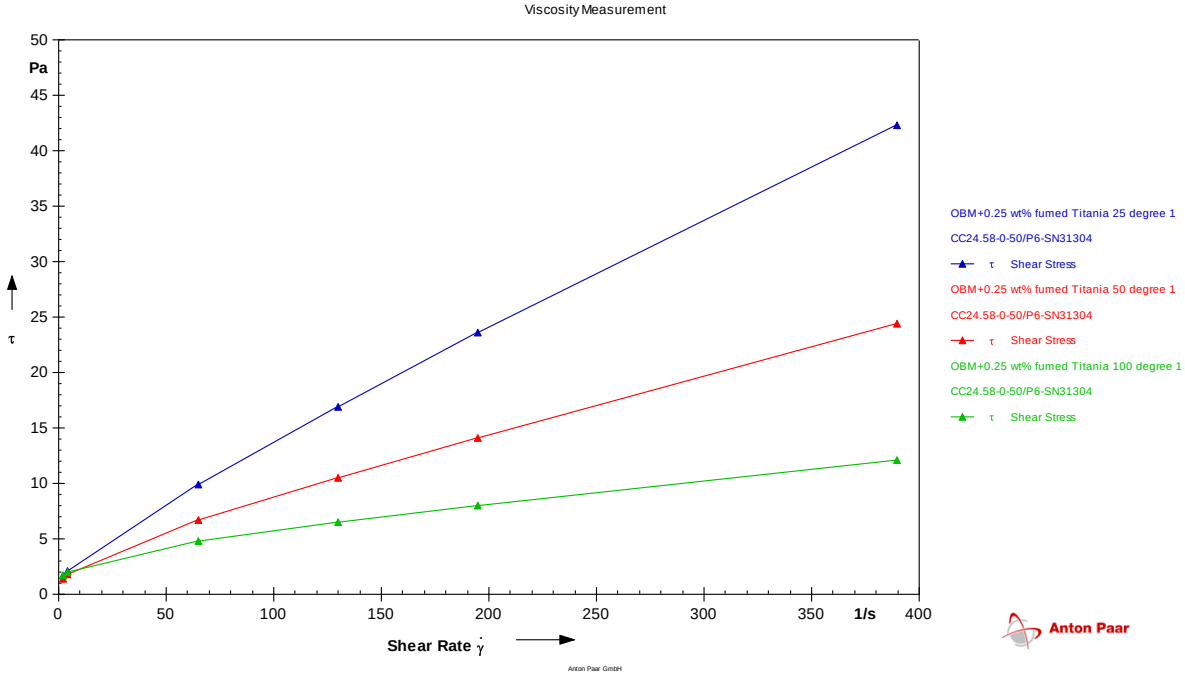

Figure 4.19: Rheological measurements of titania-based mud.

Investigating the effect of increasing particle concentration on rheology behavior of the fluid at a specific temperature is another interesting feature of this test. In this analysis, silica NPs

added fluids were compared to reference OBM at 50°C. As illustrated in the curves of Figure 4.20, shear stress is increasing with the added NPs.

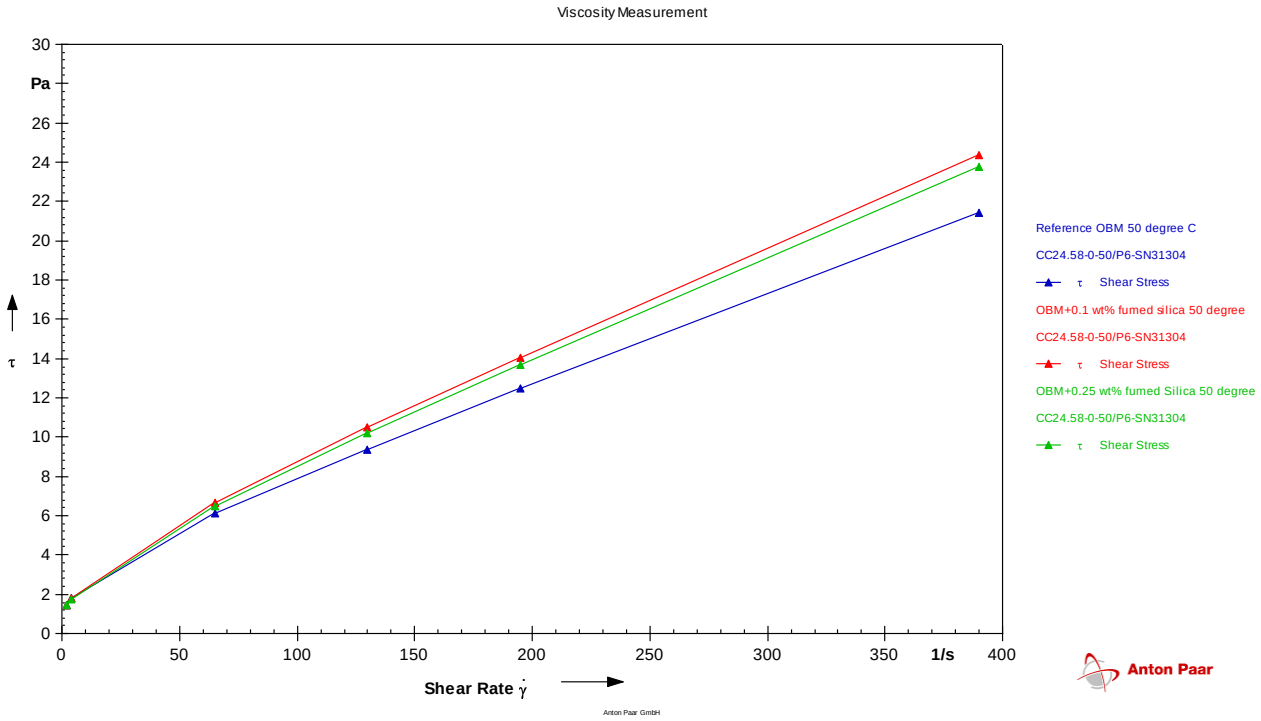

Figure 4.20: Comparison of rheological behavior of silica-based mud with the reference OBM at 50°C.

In this chapter, only the main results were described. However, during the experiments with MCR as well as POD apparatus, large quantity of raw data were generated. Some of the relevant data was summarized in the appendices, whereas, all data from the experiments were additionally attached to this thesis.

4.4. Limitation of the results

During the testing with the MCR and POD apparatus some errors can affect the results of the experiments. In this section, firstly, the errors associated with MCR tribology measurements and MCR viscometer measurements were outlined and later, errors related to the POD apparatus were exemplified.

The first relevant error with MCR tribology measurements is humidity that was not involved into the account. During the experiment times, the weather outside was not stable and with

changing the weather condition humidity was also changed. Therefore, all tribological tests with the MCR rheometer were repeated two times to maintain reliability.

Another error with the MCR tribology measurements could be related to the small volume of fluid used in the tests. When the temperature reached up to the 100°C, fluid might have dehydrated and this could result in change of lubrication properties of the tested fluid.

During the rheological measurements rheological properties could change with respect to the increased temperature such as 75°C and 100°C. The main reason is that some components inside of the tested sample could be dehydrated in these high temperatures.

In the POD apparatus, the waiting time for to reach desired temperature of tested fluid is long. In higher temperatures such as 75°C, the tested fluid can be partially dehydrated which may result in change in rheological and lubrication behavior of the fluid sample.

Finally, during the experiment, the heating spiral of POD apparatus can touch the fluid cup and may cause additional friction recording, however, this is low chance and almost was not happened in this thesis experiments.

5. Discussion

Present work has examined the effect of NP added OBM on reducing the friction factor during drilling operation. MCR and POD apparatus were used to investigate the lubricants and detailed analysis of the tribological properties. This chapter discusses the achieved experimental results, economic analysis of adding nanoparticle. It also provides some recommendations for the future work on this subject.

5.1. Evaluation of the results

The first experiments were performed with the MCR. The results which matched mostly with the theory were chosen for the experiments in the pin-on-disk apparatus. However, the values of friction coefficient taken from the MCR were not exact and reliable values. There can be several explanation for this problem: (1) The mud volume used in the MCR tribology measuring cell was 2 ml and results from this test can be unreliable where tribology properties can be presented wrong by the program. (2) The humidity factor was ignored all the time. This was confirmed by doing the experiments two times in different days, and the results were differed from each other, and finally (3) before each the experiment zenith ball distance was set to 1 mm. however, during the testing it was fluctuated and this may cause wrong interpretation of results. Due to the instability of the MCR tribology results, only the differences in the values of the friction were considered for further analysis with the pin-on-disk.

In Figure 4.1 and 4.2, friction coefficients obtained by silica and titania-based mud were plotted versus particle concentration at pre-determined values of temperature for the experiment. According to the figures, friction factor did not change significantly with 0.1 weight% silica and titania added fluids at the temperature of 50°C. Unlike the fluids with 0.1 weight% of silica and titania additives, 0.25 weight% of these NPs showed considerable reduced friction at the same temperature. Each NP was mixed within the separate sample of the same original mud having the weight of 100 g. The concentration of 0.1 weight% was too small to be mixed compared to 0.25 weight%; therefore, the results of 0.1 weight% of silica added fluids showed more or less similar behavior as the reference OBM, while 0.25 weight% of silica indicated a more reduced value compared to the reference, i.e. more lubrication.

Additionally, increasing the concentration of silica NPs in the fluid above 0.25 weight% and 50°C showed higher value of friction coefficient than the reference. This is supported by the theoretical fact that increasing of both the particles in the mud, and the temperature results in an increase in friction. This was not valid for the titania added mud, where it showed reduction in friction for the 0.5 weight% added fluid as well. This can be explained as a ball bearing effect of titania NPs and forming of smear film property of the titania NPs in high temperature.

As it is discussed previously, the experiments for the POD and MCR apparatus were respectively done with the mud sample of 100 and 2 ml. The increased value of mud viscosity in addition to the dehydration of the mud sample at 100°C, in the experiment with POD, confirmed that the quality of the sample is not convenient enough for the experiment. This is also true for the MCR as it uses less value of mud sample. So, no result is discussed for the experiment in this temperature.

Sliding speed effect over the friction coefficient is an interesting case to discuss. Since 100 measurement points were set to the program, and friction test were taken 5 minutes in each speed interval, mud volume used in the test was too small and tribological behavior can be interpreted wrong. Considering the fact of obtaining inaccurate results from the MCR, no further interpretation could be stated for the sliding speed effect.

To obtain promising results and confirm some unreliable results after MCR, triobological tests were performed with the POD apparatus. The tribological experiments were conducted at least two times in terms of reproducibility of the experimental data under 10 N and 120 RPM.

The sudden increase in the friction factor, illustrated in Figure 4.7, can be justified with this fact that the scratched materials fill the wear track which increase the friction. This was not seen in the case of adding NPs to the OBM thanks to the smoothing effect.

Based on the results of the MCR, there have been coupling effect between temperature and NPs where the friction coefficient fluctuates with the increase in temperature. Since these results can be wrong with MCR, the tests with the POD apparatus were performed in different chosen temperatures to confirm this fact. Both silica and titania-based mud with the concentration of 0.1 and 0.25 weight% showed reduction in friction at 50°C. However, at the temperature of 75°C, reduced frictions were recorded for the titania added fluids unlike the one from the silica-based fluids. This proves coupling effect between NPs and temperature which means change in friction factor with respect to the temperature with NPs added fluids

depending on the concentration, properties, surface area and the type of the NPs. Adding nanoparticles to the reference OBM reduced the standard deviation and stabilized the friction movement compared to those in reference OBM.

As presented in the theory section, higher temperature leads to lower viscosity and this results in increase in friction. Titania added fluids contradict this fact, as the friction follows a decreasing trend in the temperatures above 50°C. This is due to the dehydration of the tested fluid. Additionally, the rolling medium of nanoparticles acting between rubbing surfaces can be another reason for this behavior. In 2006, Wu et. Al [4] achieved the similar results by performing experimental analysis of tribological properties of lubricating oils with NP additives.

Unlike silica, titania has an ability to form smear film at higher temperatures between the rubbing surfaces which reduces friction factor and protects disk surface from wearing. However, establishing of this coating is not easy and therefore, possibility of other lubrication mechanisms should be investigated.

To prefer silica NPs over the silica micro-particles which provided by ZEB at NTNU, tribology measurements were performed with the same conditions. Based on the results provided in the previous section, micro-silica particles with the concentrations of 0.1 and 0.25 weight% showed reduction in friction at 50°C and increase in friction at 75°C similar to those from the silica NPs. However, silica NPs contained OBM showed better results and significant reduced friction than silica micro-particles. The reason could be the bigger size of the micro-silica compared to silica NPs which was around 300 nm. After visual observations of disk samples, more loss volume was noticed with the silica micro-particles than silica NPs. This also supports the fact presented in the theory stating that increasing the particle size enlarges the value of the friction factor. This results in higher loss volume from the disk due to the abrasive wear mechanism. Based on these results, NPs are likely to be preferred to the micro-particles in the research.

For further study, tested disk samples were analyzed on the optical 3D confocal microscope to calculate loss volume. No scar depth was observed by the microscope. This shows that how OBM including NPs added fluids are good lubricator and reduce the friction between rubbing surfaces. The images taken from the 3D optical microscope are shown in Appendix B.

Since POD is considered to be reliable and accurate, some similar experiments were recently done using WBM with and without the same amount of NPs in it. The results are compared to those with OBM in Table 5.1. Obviously, values of friction factor for OBM and WBM are differed significantly from each other, therefore, reduced friction factor were mentioned with the percentage for easy comparison of the effect of NPs on both WBM and OBM.

Table 5.1: Comparison of friction factor obtained by OBM and WBM at 50°C.

Fluid name	Friction factor	Reduction in friction	Fluid name	Friction factor	Reduction in friction
Reference OBM	0.157	0%	Reference WBM	0.57	0%
0.1 wt% silica	0.131	17%	0.1 wt% silica	0.517	9.2%
0.25 wt% silica	0.083	47%	0.25 wt% silica	0.418	26.7%
0.1 wt% titania	0.135	14%	0.1 wt% titania	0.503	11.8%
0.25 wt% titania	0.115	26%	0.25 wt% titania	0.492	13.7%

As shown in the table, the best results were achieved with the 0.25 weight% of both silica and titania added fluids in both cases. In addition to that, the values of the friction factor obtained by the WBM is much higher than OBM. This is because of the OBM is better lubricator than WBM.

For better analysis of the results, lowest value of friction factor was taken for OBM and highest one for NP-based mud. For example, 0.25 weight% of silica-based mud at the temperature of 50°C showed 47% reduction in friction by taking the highest value of this silica-based mud. However, if the lowest value of 0.25 weight% concentration silica added fluid was taken i.e. if test 1 was taken for the comparison, the friction factor would be reduced by 63%. Therefore, the values of the friction factor shown in this thesis work were the minimum values, whereas, friction reduction even can be higher in reality.

Moreover, viscometer measurements were performed at temperatures of 25, 50 and 100°C and fluid volumes used in the test was around 10-11 ml. There could be dehydration at 100°C, however that was not noticed during the experiments. The reason was small amount of mud volume used in the test and the short testing time.

Adding NPs did not affect the rheological behavior of the mud significantly, as it is presented in the result section. All the samples ended up with having some trend of changing as Herschel-Buckley model. The slight increase of viscosity of the samples after adding the NPs gives this

idea that NPs can be applied as viscosifier in the experiments. Although, this fact needs to be proved in some other work due the limited time specified for this work.

5.2. Evaluation of the fluids

This subsection presents the economic analysis of adding NPs to the sample done in this work. The given values of drilling fluid density and volume together with NP concentration in the mud, its density and price are used for this analysis. These values are presented in Table 5.2:

Table 5.2: Given parameters before analyses.

Name	Silica		Titania		Drilling Fluid
Concentration (wt%)	0.1	0.25	0.1	0.25	-
Volume (m3)	-		-		500
Density (kg/m3)	50		50		1200
Cost (USD/kg)	50		500		-

The weight of NP is calculated as

$$W_{NP} = \rho_{DF} \cdot V_{DF}.C_{NP}/100 \tag{5.1}$$

where:

$W_{NP} =$ weight of nanoparticle, kg

$\rho_{DF} =$ density of drilling fluid, kg/m^3

$C_{NP} =$ concentration of nanoparticle, weight%

$V_{DF} =$ Volum of drilling fluid, m^3

Total price of the NP is obtained by

$$P_{NP} = W_{NP} \cdot C'_{NP} \tag{5.2}$$

where:

$P_{NP} =$ total cost of nanoparticle, USD

$C'_{NP} =$ cost of nanoparticle per kilogram, USD/kg

The results are summarized in the table below.

Table 5.3: Economic calculations.

Silica-based drilling fluids				Titania-based drilling fluids			
Concentration, wt%	Weight, kg	Volume, m3	Price, USD	Concentration, wt%	Weight, kg	Volume, m3	Price, USD
0.1	600	12	30000	0.1	600	12	300000
0.25	1500	30	75000	0.25	1500	30	750000
0.5	3000	60	150000	0.5	3000	60	1500000

As shown in Table 5.3, increasing NP concentration and density requires more financial investment. Since silica NPs are 10 times cheaper than titania NPs, they are more preferable to titania. Considering the results of 0.25 weight% silica added fluids at a temperature of 50°C, the cost of NPs used in 500 m^3 of drilling fluid is 75000 USD. Addition to that, 47% reduced friction was obtained with these concentrations of silica meaning that drilling length is roughly increased by 47%. Therefore, to make sure of using NPs in this situation, sensitivity analyses is required.

Moreover, silica NPs is a safe matter in nanometer scale. These particles already applied to the industries such as cosmetic, constriction materials, medicine and so on. Even though titania particles are also used in some industries, however application of these particles are in debate in terms of HSE [34][35]. Considering the fact of application of NPs in drilling fluids is in its infancy level; therefore, more research can be done in titania toxicity.

To summarize, even though the experiments in this work as well as the previous work done with the WBM [13] are successful, there is still a need to do more research in this area.

6. Conclusion

In this thesis, the effect of nanofluids on reduced friction was investigated and based on the experimental results and previous work in this area, the following main points could be drawn:

- Nanofluids promise reduction in friction between rubbing surfaces. The expected reduction depends on the selected nanoparticles and concentration of the nanoparticles in the fluid.
- There is coupling effect between nanoparticles and temperature which depending on the types of nanoparticles and physical properties used in the drilling fluid.
- Silica and titania nanoparticles used as an additive in OBM show good friction reduction and stabilized frictional movement at the temperature of 50°C.
- The best results in the friction test were achieved with the concentration of 0.25 weight% silica added fluid where the friction factor was reduced to the minimum of 47%.
- Since the friction factor is directly proportional to the size of the particles, silica nanoparticles are more effective than silica micro-particles in reducing the friction factor due to their smaller size.

7. Future works

Since application of nanoparticles in drilling is in its infancy level, more work should be done before commencement. During this work significant reduction were achieved with the titania and silica nanoparticles. However, more works are needed to be done to explore nanoparticles as a potential friction reducing agent during drilling. Further investigations could be conducted on friction reduction such as:

- Concentration of silica and titania higher than 0.25 weight%.
- Higher sliding speeds on pin-on-disk apparatus.
- Sensitivity analysis.
- Higher values of normal load than 10 N.
- More research on HSE of titania and silica.
- Avoid using the same mud.
- Avoid keeping the mud for a long time.
- Equal or lower than 75 °C not recommended.
- Viscosifying effect of nanoparticle.

8. Bibliography

[1] H. Geir, W. Andrew, L. Lingyun, M. M. Husein and F. Z. Muhammed, *Innovative Nanoparticle Drilling Fluid and Its Benefits to Horizontal or Extended Reach Drilling,* Alberta, Canada: Society of Petroleum Engineers, SPE 162686, 2012.

[2] W. Jianyang, H. Jianying, T. Ole and Z. Zhang, *Effect of Nanoparticles on Oil-Water Flow in a Confident Nanochannel: a Molecullar Dynamics Study,* Noordwijk, The Netherlands, : Society of Petroleum Engineers, SPE 156995, 2012.

[3] K. Xiangling and O. Michael M., *Application of Micro and Nano Technologies in the oil and gas industry - An Overview of the Recent Progress,* Abu Dhabi: Society of Petroleum Engineers, SPE 138241, 2010.

[4] Y. Y. Wu, W. C. Tsui and T. Liu, *Experimental analysis of tribological properties of lubricating oils with nanoparticle additives,* Taiwan: Science Direct, 2006.

[5] E. Broni-Bediako and R. Amorin, "Effects of Drilling Fluid Exposure to Oil and Gas Workers Presented with Major Areas of Exposure and Exposure Indicators," *Research Journal of Applied Sciences, Engineering and Technology: 710-719,* 2010.

[6] HWU, "Drilling Engineering, Lecture Material," Edinburg, UK, 2009, pp. 358-363.

[7] M. Hossain and A. Al-Majed, "Fundamentals of Sustainable Drilling Engineering," John Wiley & Sons and Scrivener Publishing Company, Austin, TX 78702, 2012.

[8] S. N. Shah, P.E., N. H. Shanker and C. C. Ogugbue, "Future Challanges of Drilling Fluids and Their Rheological Measurements," in *AADE Fluids Conference and Exhibition*, Houston, Texas, 2010.

[9] M. Amanullah and A. M. Al-Tahini, *Nano-Technology- Its Significance in Smart Fluid Development for Oil and Gas Field Application,* AlKhobar, Saudi Arabia: Society of Petroleum Engineers, SPE 126102, 2009.

[10] D. W.-M. Liu and D. X.-B. Wang, "Nanoparticle-based lubricant additives," in *Springer-Verlag Berlin Heidelberg*, 2012.

[11] E. Kaarstad, B. Aadnoy and T. Fjelde, *A Study of Temperature Dependent Friction in Wellbore Fluids,* Amsterdam: Society of Petroleum Engineers or the International Association of Drilling Contractors, SPE/IADC 119768, 2009.

[12] G. W. Stachowiakl and A. W. Batchelor, Engineering Tribology, Oxford, OX5 1GB, UK: Butterworth-Heinemann, 2014.

[13] C. Jahns, "Friction Reduction by using Nano-Fluids," NTNU, Trondheim, Norway, 2014.

[14] S. Shaffer, "Bruker Corporation," Bruker, 29 January 2013. [Online]. Available: http://www.bruker.com/fileadmin/user_upload/8-PDF-Docs/SurfaceAnalysis/TMT/Webinars/Tribology_101_Webinar-1_Intro_and_Basics_29-Jan-2013.pdf. [Accessed 4 April 2014].

[15] J. R. Jones, "Lubrication, Friction, and Wear," NASA, Hampton, Virgina 23365, 1971.

[16] P. Skalle, Drilling Fluid Engineering, Trondheim: Pål Skalle & Ventus Publishing ApS, 2011.

[17] Baker Hughes, Drilling Fluids reference manual, 2006.

[18] "Tececo PTY. Ltd.," [Online]. Available: http://www.tececo.com/technical.rheological_shrinkage.php. [Accessed 15 May 2014].

[19] N. Nader and E. Milad, *THE POTENIAL IMPACT OF NANOMATERIALS IN OIL DRILLING INDUSTRY*, Brno, Czech Republic: NANOCON, 2012.

[20] S. A. Adelye, A.-M. Abdulaziz and H. Enamul, *Drilling Fluids: State of The Art and Future Trend*, Cairo, Egypt : Society of Petroleum Engineers, SPE 149555, 2012.

[21] S. Robello, *Friction Factors: What are They for Torque, Drag, Vibration, Bottom Hole Assembly and Transient Surge/Swab Analyses?*, New Orleans, Louisiana: IADC/SPE 128059, 2010.

[22] "Copyright © 2013 Petroleum.co.uk . All Rights Reserved," [Online]. Available: http://www.petroleum.co.uk/. [Accessed 08 May 2014].

[23] G99-05 (reapproved 2010) DIN standard: DIN50324. International Standardization G99 - 05 (Reapproved 2010). Standard test method for wear testing with a pin-on-disk apparatus designation: Copyright by ASTM International, 2010., Developed by Subcommittee: G02.40.

[24] "Tribology - Heat Treatments - Q.A.S Laboratory," [Online]. Available: http://triblab.teipir.gr/en/pg000.html. [Accessed 23 May 2014].

[25] Anton Paar, *Instruction Manual: Tribology Measuring Cell T-PTD200,* Document nr: B98ib052EN-L., 2012.

[26] George R. Gray Ryen Caenn, H.C.H Darley, Composition and Properties of Drilling and Completion Fuids, 2011: Gulf Professional Publishing - an imprint of Elsevier, 6th edition.

[27] "Viscopedia," A free ensiclopedia for viscosity, [Online]. Available: http://www.viscopedia.com/methods/measuring-principles/. [Accessed 2014 10 June].

[28] M. Jan and N. J. Wagner, Colloidal Suspension Rheology, Cambridge University Press, 2012.

[29] Anton Paar, MCR Series, Modular Compact Rheometer MCR 52/102/302/502 Smartpave EC-Twist 302 / EC-Starch 302, Instruction Manual: Document nr: C92IB001EN-C, 2011.

[30] MI SWACO , "http://www.slb.com/services/miswaco/services/completions/reservoir_drill_in_fluids/versapro_ls.aspx," A Schlumberger Company. [Online]. [Accessed 16 June 2014].

[31] Product Information Datasheet, "Elkem nanosilica 999," [Online]. Available: http://www.elkem.com/Global/ESM/quality-safety/product-data-sheets/polymer-applications/nano-silica999-product-data-sheet.pdf. [Accessed 10 June 2014].

[32] Hydrophilic fumed silica, [Online]. Available: https://www.aerosil.com/lpa-productfinder/page/productsbytext/detail.html?pid=1830&lang=en. [Accessed 10 June 2014].

[33] Hydrophilic fumed metal oxides, [Online]. Available: https://www.aerosil.com/product/aerosil/en/products/hydrophilic-fumed-metal-oxides/pages/default.aspx. [Accessed 11 June 2014].

[34] S. Alison and S. G. Karen, *Toxicological review of the possible effects associated with inhalation and dermal exposure to drilling fluid production streams,* Edinburgh: IOM, 2011.

[35] K. Mohamed, K.-S. Malika, P. C. Jean, C. Nathalie and B. Faïza, *Drilling Fluid Technology: Performances and Environmental Considerations,* INTECH, 2010.

9. Appendices

Appendix A

Table A.1: Mean values of friction factor for each speed interval of reference OBM.

RPM	25°C	50°C	100°C
3	0.215	0.224	0.178
6	0.209	0.262	0.304
100	0.238	0.293	0.341
200	0.237	0.267	0.288
300	0.24	0.279	0.247
600	0.231	0.241	0.226
Average Fc	0.228	0.261	0.264

Table A.2: Mean values of friction factor for each speed interval of 0.1 weight% of silica-based mud.

RPM	25°C	50°C	100°C
3	0.218	0.221	0.203
6	0.221	0.231	0.305
100	0.234	0.239	0.335
200	0.250	0.250	0.291
300	0.255	0.243	0.289
600	0.245	0.232	0.236
Average Fc	0.237	0.236	0.276

Table A.3: Mean values of friction factor for each speed interval of 0.25 weight% of silica-based mud.

RPM	25°C	50°C	100°C
3	0.210	0.245	0.168
6	0.212	0.246	0.241
100	0.250	0.250	0.301
200	0.247	0.263	0.284
300	0.228	0.267	0.252
600	0.231	0.235	0.227
Average Fc	0.230	0.251	0.245

Table A.4: Mean values of friction factor for each speed interval of 0.5 weight% of silica-based mud.

RPM	25°C	50°C	100°C
3	0.224	0.235	0.254
6	0.219	0.224	0.328
100	0.229	0.251	0.322
200	0.250	0.257	0.304
300	0.249	0.239	0.268
600	0.246	0.227	0.223
Average Fc	0.236	0.239	0.283

Table A.5: Mean values of friction factor for each speed interval of 0.1 weight% of titania-based mud.

RPM	25°C	50°C	100°C
3	0.214	0.278	0.169
6	0.221	0.278	0.221
100	0.231	0.264	0.282
200	0.235	0.261	0.232
300	0.229	0.251	0.245
600	0.236	0.224	0.194
Average Fc	0.228	0.259	0.224

Table A.6: Mean values of friction factor for each speed interval of 0.25 weight% of titania-based mud.

RPM	25°C	50°C	100°C
3	0.187	0.209	0.208
6	0.193	0.209	0.287
100	0.210	0.226	0.293
200	0.199	0.239	0.258
300	0.214	0.235	0.228
600	0.205	0.201	0.196
Average Fc	0.201	0.220	0.245

Table A.7: Mean values of friction factor for each speed interval of 0.5 weight% of titania-based mud.

RPM	25°C	50°C	100°C
3	0.211	0.232	0.157
6	0.208	0.224	0.246
100	0.207	0.264	0.319
200	0.227	0.278	0.266
300	0.234	0.268	0.245
600	0.234	0.232	0.194
Average Fc	0.220	0.249	0.238

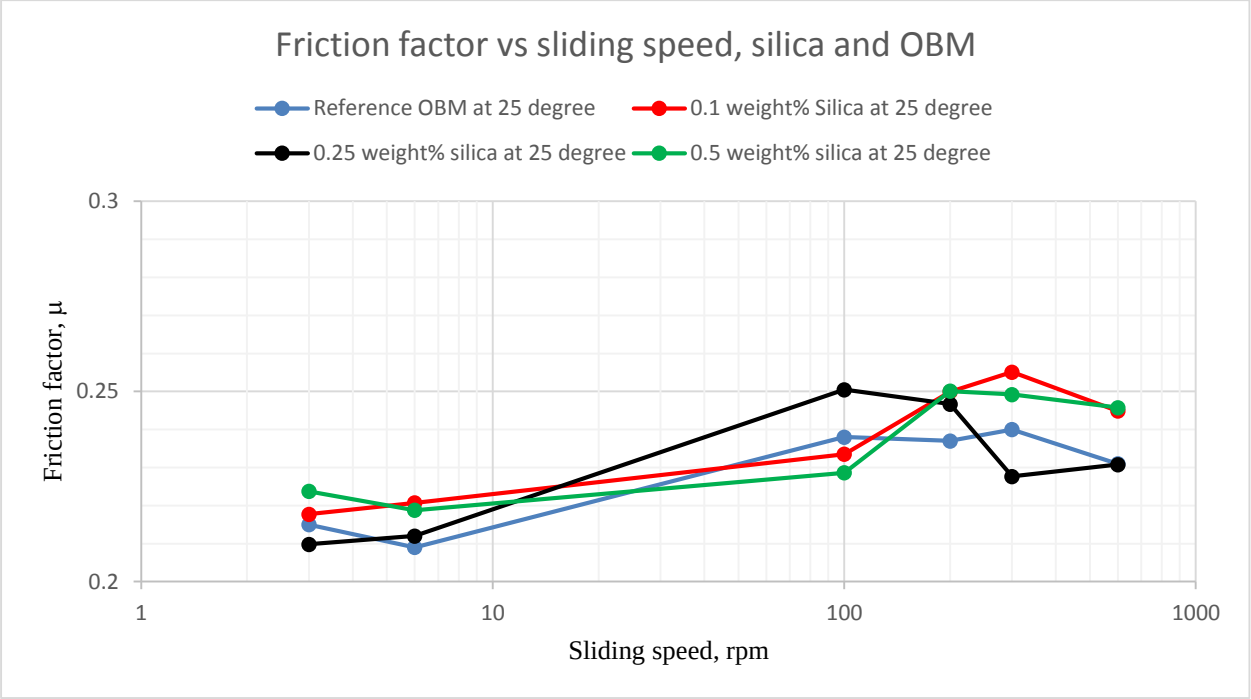

Figure A.1: Dependence of friction factor on the sliding speed with the silica-based mud at 25°C.

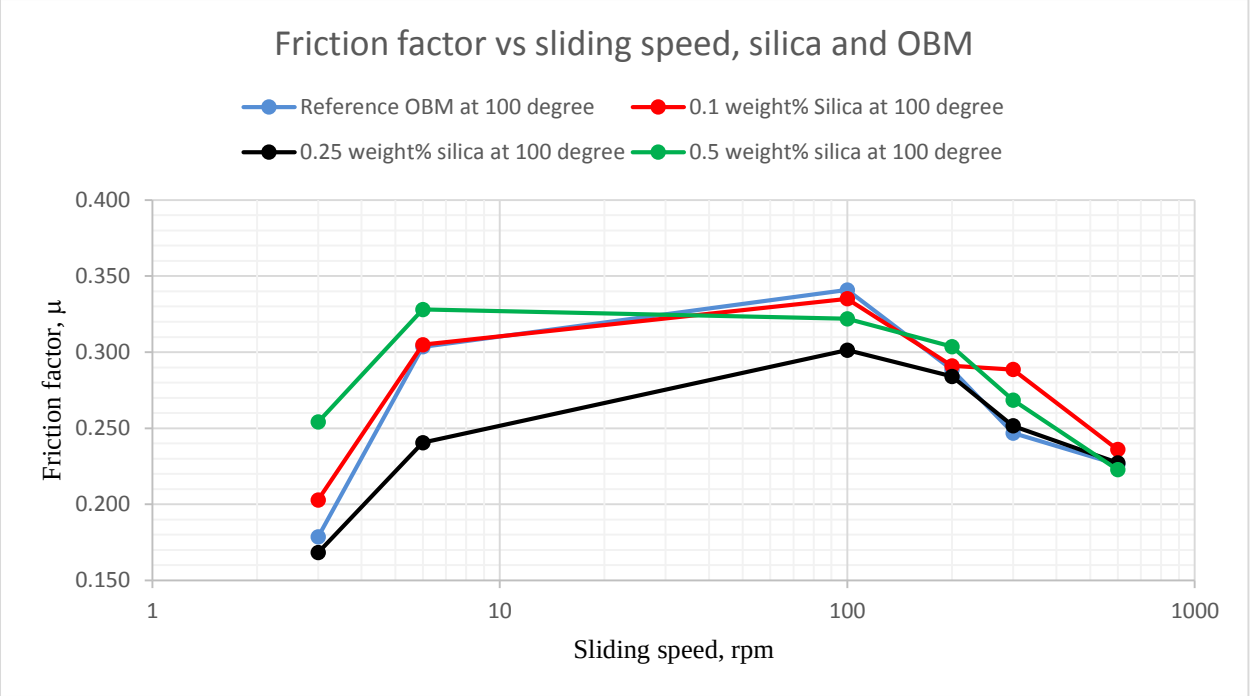

Figure A.2: Dependence of friction factor on the sliding speed with the silica-based mud at 100°C.

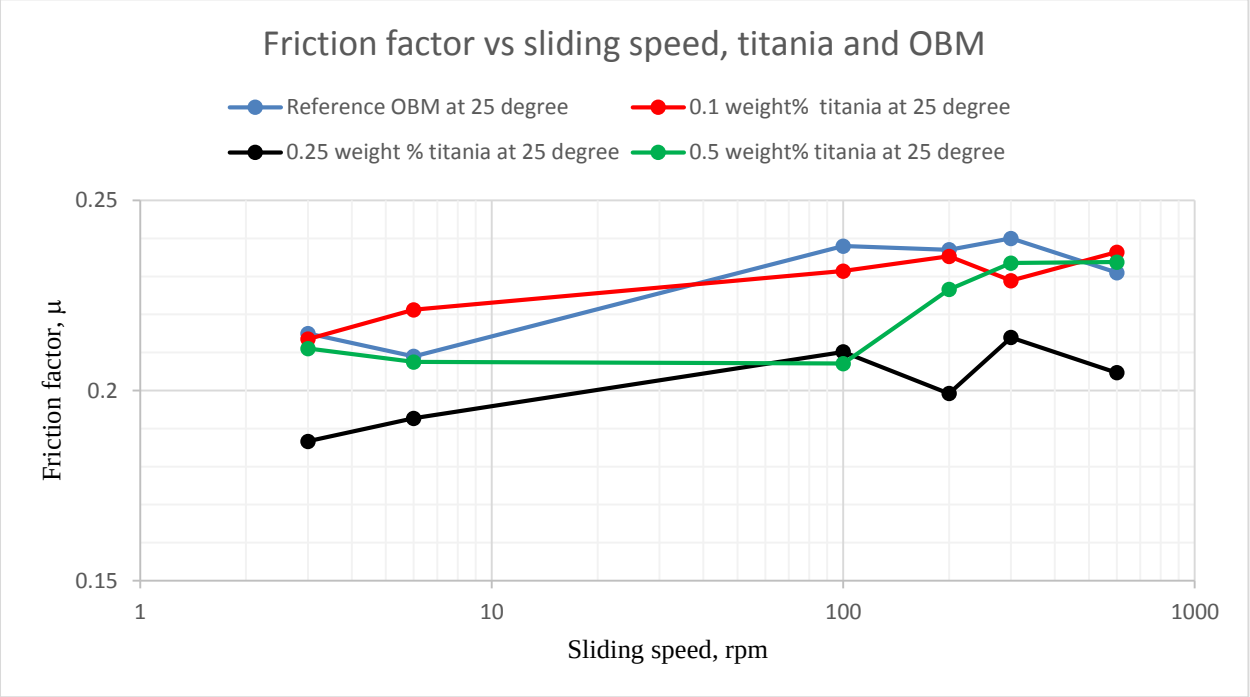

Figure A.3: Dependence of friction factor on the sliding speed with the titania-based mud at 25°C.

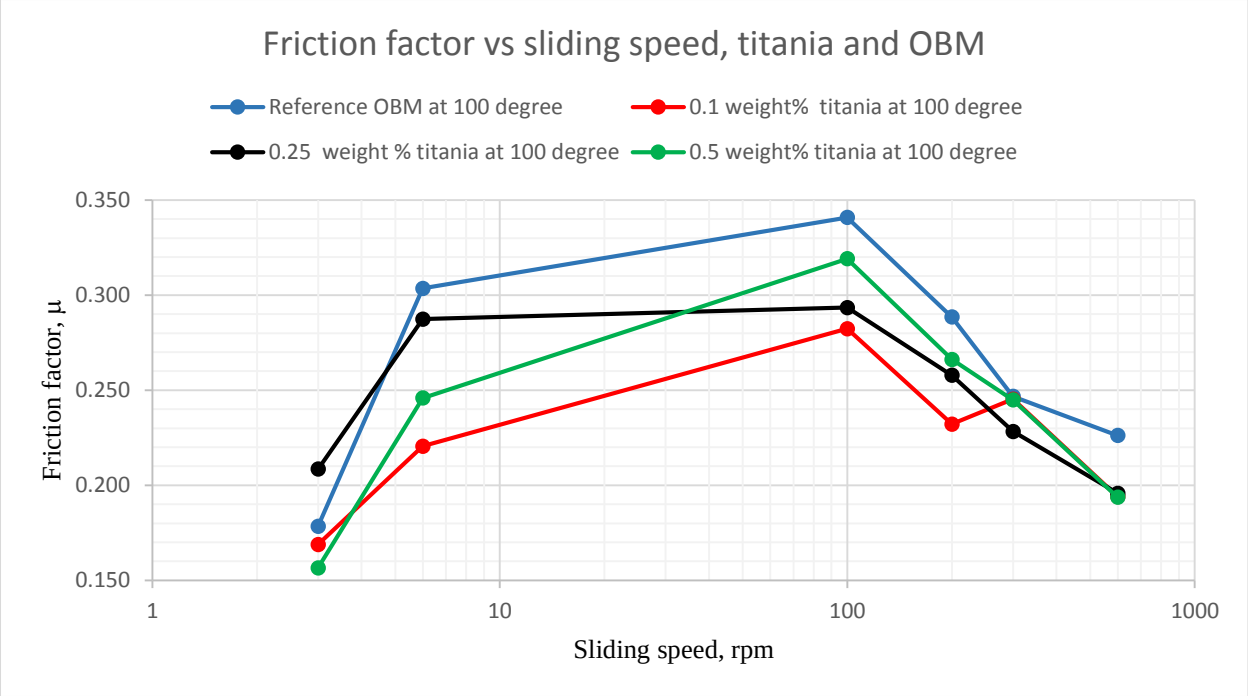

Figure A.4: Dependence of friction factor on the sliding speed with the titania-based mud at 100°C.

Appendix B

Table B.1: Comparison of nanoparticle based muds with the reference OBM.

Mean Friction Factor							
	Reference OBM	Silica		Titania		Micro-silica	
Temperature	no added particles	0.1 wt%	0.25 wt%	0.1 wt%	0.25 wt%	0.1 wt%	0.25 wt%
50°C	0.1571	0.1305	0.0828	0.1348	0.1155	0.1319	0.1347
75°C	0.1434	0.1995	0.1446	0.1203	0.1270	0.1332	0.2145

Figure B.1: A) OBM at 100°C (dehydrated), **B)** OBM at 50°C.

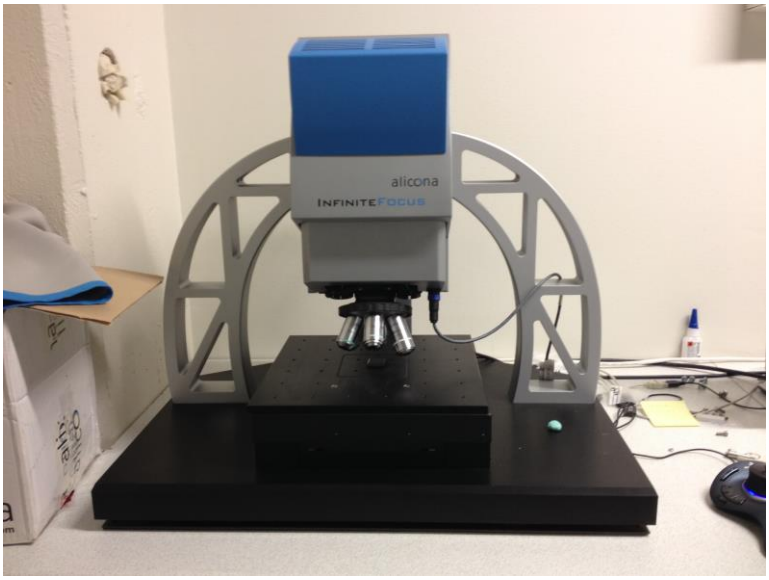

Figure B.2: Optical 3D confocal microscope.

Figure B.3: Example of scratched sample with the reference OBM at 50°C.

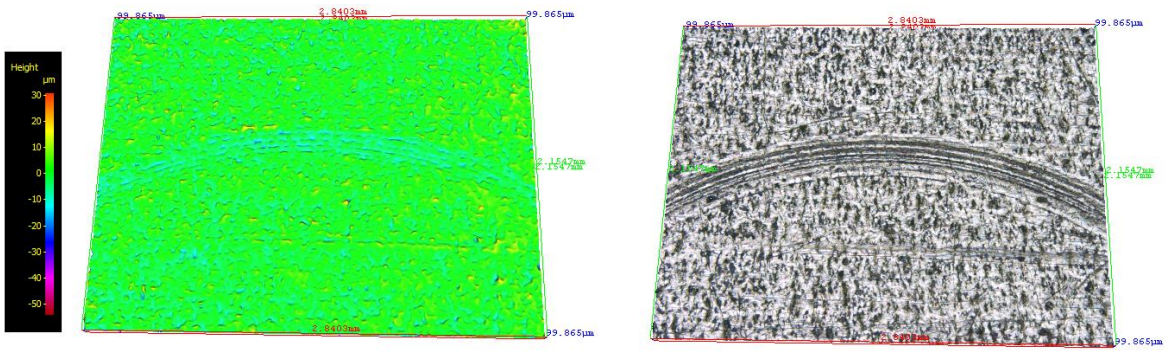

Figure B.4: İmage of scratched sample created with 0.1 weight% of silica-based mud at 50°C.

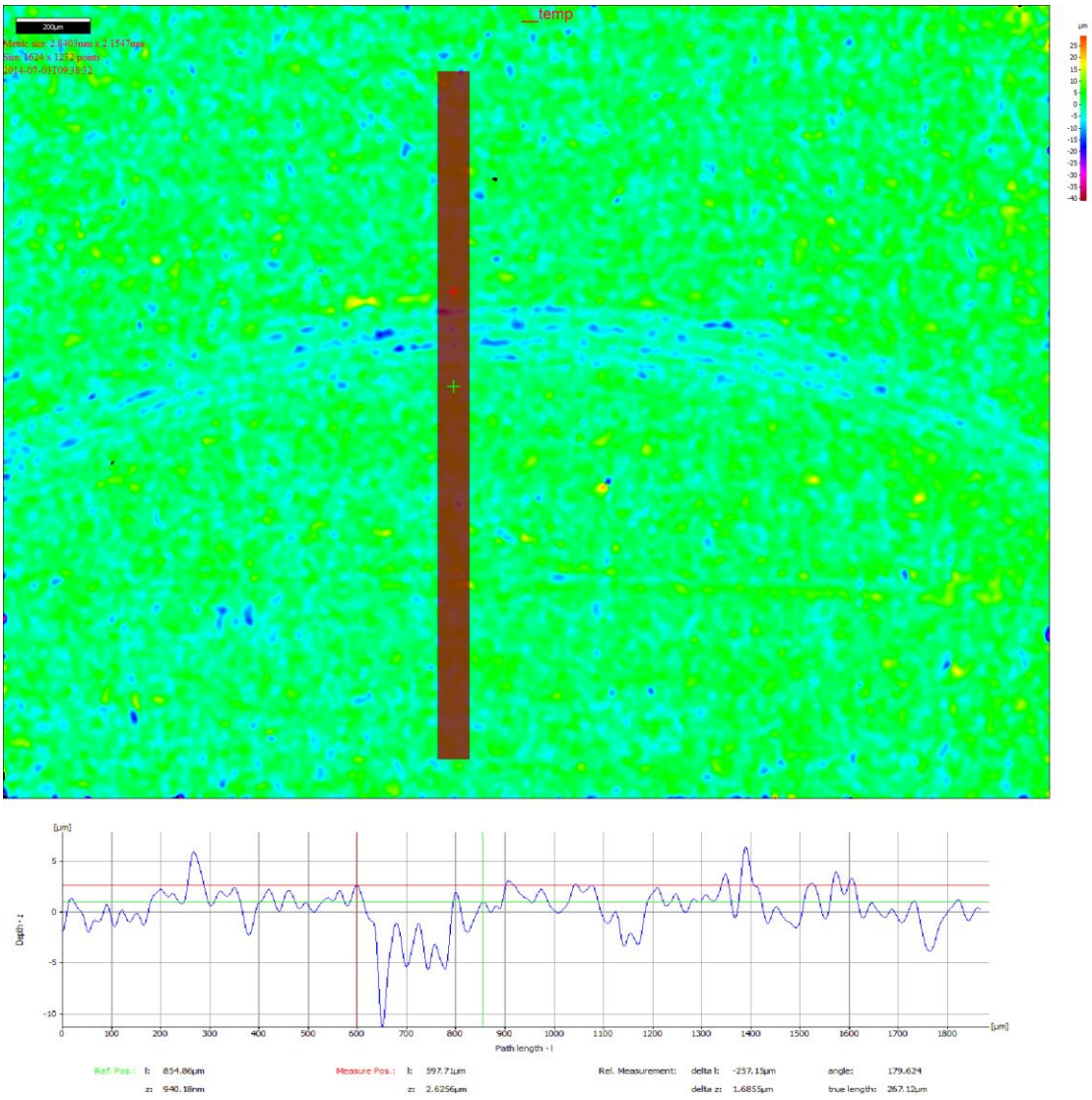

Figure B.5: Profile diagram of the scratched sample with 0.1 weight% silica-based mud at 50°C.

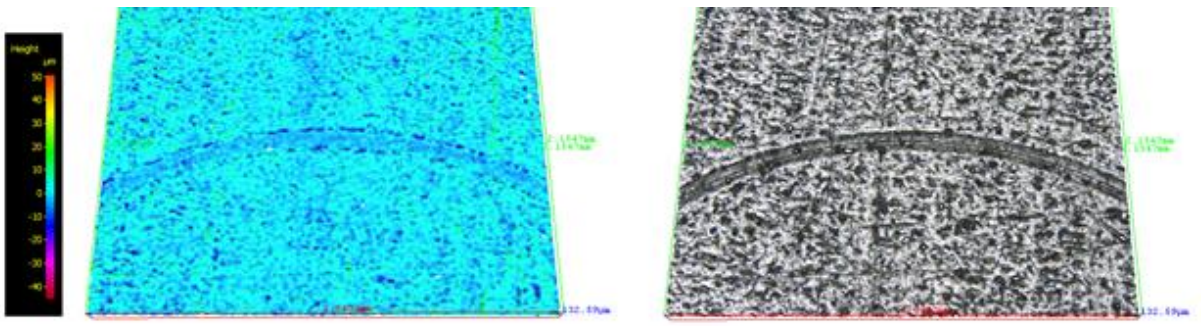

Figure B.6: İmage of scratched sample created with 0.25 weight% of silica-based mud at 50°C.

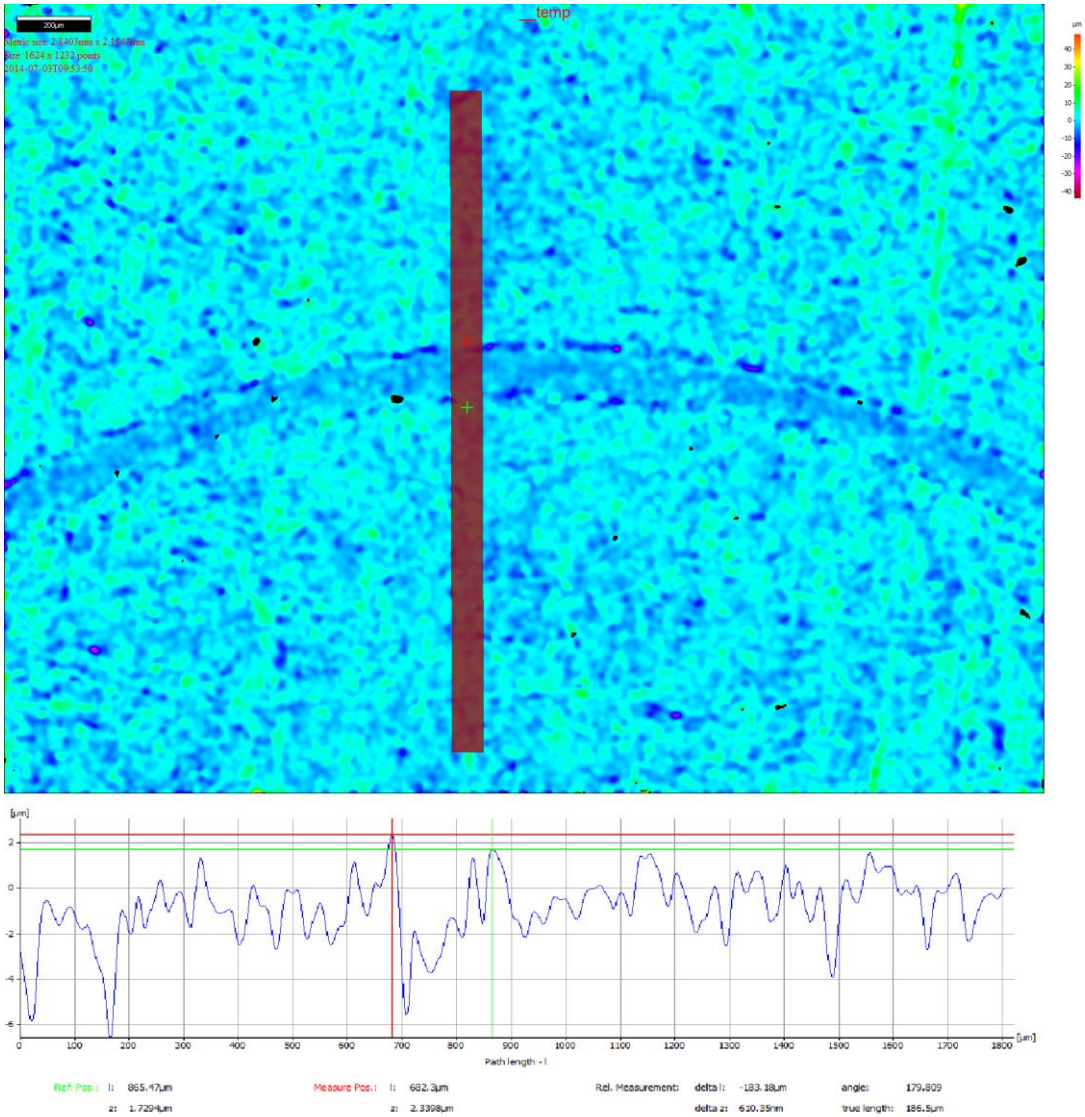

Figure B.7: Profile diagram of the scratched sample with 0.25 weight% silica-based mud at 50°C.

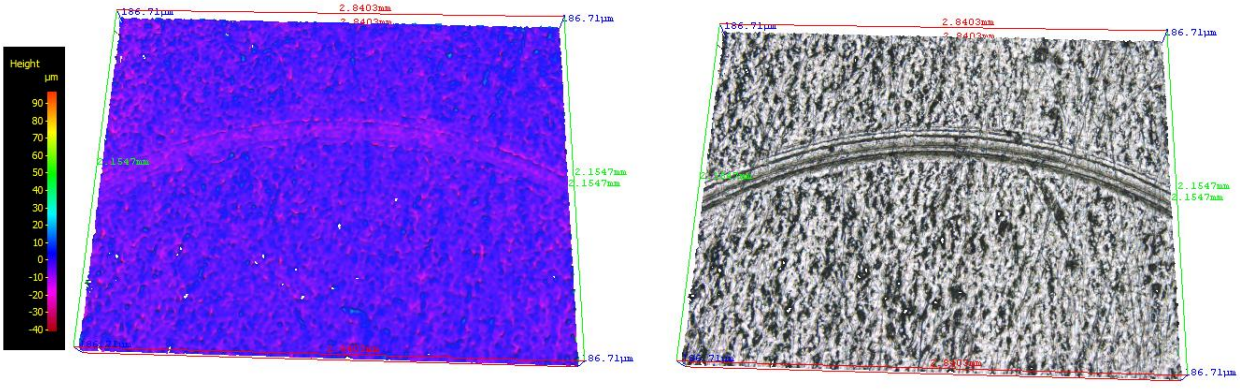

Figure B.8: İmage of scratched sample created with 0.25 weight% of titania-based mud at 50°C.

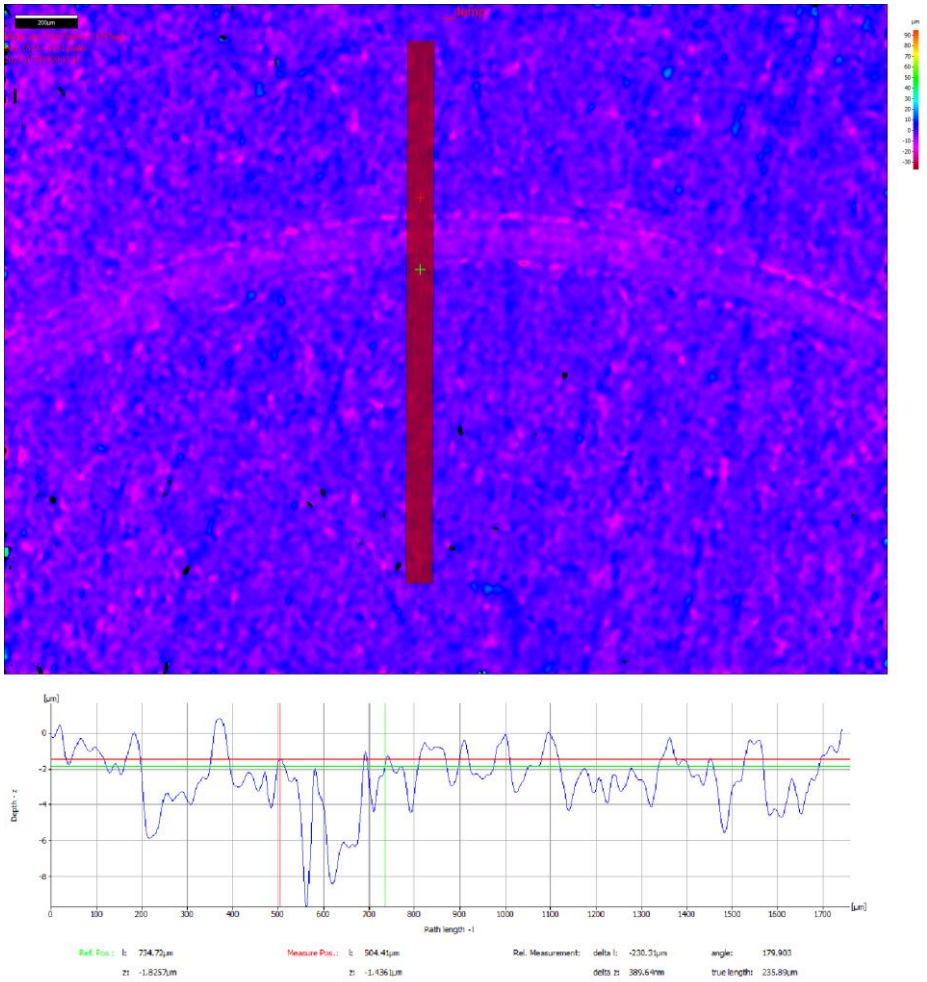

Figure B.9: Profile diagram of the scratched sample with 0.25 weight% titania-based mud at 50°C.

Appendix C

Table C.1: MCR viscometer data of reference OBM at 25°C.

Meas. Pts.	Shear Rate	Shear Stress	Viscosity	Speed	Torque
-	[1/s]	[Pa]	[Pa·s]	[1/min]	[µNm]
1	1.95	1.65	0.845	3	111
1	3.9	2.08	0.534	6	141
1	65	9.66	0.149	100	654
1	130	16.4	0.126	200	1,110
1	195	22.8	0.117	300	1,540
1	390	40.9	0.105	600	2,770

Table C.2: MCR viscometer data of reference OBM at 50°C.

Meas. Pts.	Shear Rate	Shear Stress	Viscosity	Speed	Torque
-	[1/s]	[Pa]	[Pa·s]	[1/min]	[µNm]
1	1.95	1.47	0.753	3	99.3
1	3.9	1.77	0.455	6	120
1	65	6.09	0.0938	100	412
1	130	9.38	0.0722	200	635
1	195	12.5	0.0639	300	843
1	390	21.4	0.055	600	1,450

Table C.3: MCR viscometer data of reference OBM at 100°C.

Meas. Pts.	Shear Rate	Shear Stress	Viscosity	Speed	Torque
-	[1/s]	[Pa]	[Pa·s]	[1/min]	[µNm]
1	1.95	1.64	0.843	3	111
1	3.9	1.92	0.494	6	130
1	65	4.52	0.0696	100	306
1	130	6.09	0.0469	200	412
1	195	7.43	0.0381	300	503
1	390	11.1	0.0286	600	754

Table C.4: MCR viscometer data of 0.1 weight% of silica-based mud at 25°C.

Meas. Pts.	Shear Rate	Shear Stress	Viscosity	Speed	Torque
-	[1/s]	[Pa]	[Pa·s]	[1/min]	[µNm]
1	1.95	1.61	0.828	3	109
1	3.9	2.08	0.533	6	141
1	65	9.71	0.15	100	657
1	130	16.6	0.128	200	1,120
1	195	23.2	0.119	300	1,570
1	390	41.6	0.107	600	2,820

Table C.5: MCR viscometer data of 0.1 weight% of silica-based mud at 50°C.

Meas. Pts.	Shear Rate	Shear Stress	Viscosity	Speed	Torque
-	[1/s]	[Pa]	[Pa·s]	[1/min]	[µNm]
1	1.95	1.43	0.736	3	97.1
1	3.9	1.81	0.464	6	122
1	65	6.66	0.103	100	451
1	130	10.5	0.0808	200	710
1	195	14	0.072	300	950
1	390	24.4	0.0626	600	1,650

Table C.6: MCR viscometer data of 0.1 weight% of silica-based mud at 100°C.

Meas. Pts.	Shear Rate	Shear Stress	Viscosity	Speed	Torque
-	[1/s]	[Pa]	[Pa·s]	[1/min]	[µNm]
1	1.95	1.69	0.866	3	114
1	3.9	1.96	0.504	6	133
1	65	4.54	0.0699	100	307
1	130	6.09	0.0469	200	412
1	195	7.4	0.038	300	501
1	390	11	0.0283	600	747

Table C.7: MCR viscometer data of 0.25 weight% of silica-based mud at 25°C.

Meas. Pts.	Shear Rate	Shear Stress	Viscosity	Speed	Torque
-	[1/s]	[Pa]	[Pa·s]	[1/min]	[µNm]
1	1.95	1.7	0.874	3	115
1	3.9	2.2	0.565	6	149
1	65	10.4	0.159	100	701
1	130	17.5	0.135	200	1,190
1	195	24.3	0.125	300	1,640
1	390	43.3	0.111	600	2,930

Table C.8: MCR viscometer data of 0.25 weight% of silica-based mud at 50°C.

Meas. Pts.	Shear Rate	Shear Stress	Viscosity	Speed	Torque
-	[1/s]	[Pa]	[Pa·s]	[1/min]	[µNm]
1	1.95	1.44	0.74	3	97.5
1	3.9	1.76	0.453	6	119
1	65	6.5	0.1	100	440
1	130	10.2	0.0786	200	691
1	195	13.7	0.0702	300	925
1	390	23.8	0.061	600	1,610

Table C.9: MCR viscometer data of 0.25 weight% of silica-based mud at 100°C.

Meas. Pts.	Shear Rate	Shear Stress	Viscosity	Speed	Torque
-	[1/s]	[Pa]	[Pa·s]	[1/min]	[µNm]
1	1.95	1.65	0.847	3	112
1	3.9	1.95	0.499	6	132
1	65	4.58	0.0705	100	310
1	130	6.17	0.0475	200	418
1	195	7.53	0.0386	300	509
1	390	11.3	0.029	600	764

Table C.10: MCR viscometer data of 0.5 weight% of silica-based mud at 25°C.

Meas. Pts.	Shear Rate	Shear Stress	Viscosity	Speed	Torque
-	[1/s]	[Pa]	[Pa·s]	[1/min]	[µNm]
1	1.95	1.82	0.932	3	123
1	3.9	2.35	0.604	6	159
1	65	11.5	0.178	100	781
1	130	19.6	0.151	200	1,330
1	195	27.1	0.139	300	1,830
1	390	48	0.123	600	3,250

Table C.11: MCR viscometer data of 0.5 weight% of silica-based mud at 50°C.

Meas. Pts.	Shear Rate	Shear Stress	Viscosity	Speed	Torque
-	[1/s]	[Pa]	[Pa·s]	[1/min]	[µNm]
1	1.95	1.5	0.77	3	102
1	3.9	1.9	0.488	6	129
1	65	7.41	0.114	100	501
1	130	11.8	0.0908	200	798
1	195	15.8	0.0812	300	1,070
1	390	27.5	0.0706	600	1,860

Table C.12: MCR viscometer data of 0.5 weight% of silica-based mud at 100°C.

Meas. Pts.	Shear Rate	Shear Stress	Viscosity	Speed	Torque
-	[1/s]	[Pa]	[Pa·s]	[1/min]	[µNm]
1	1.95	1.74	0.893	3	118
1	3.9	2.03	0.52	6	137
1	65	4.94	0.0761	100	334
1	130	6.77	0.0521	200	458
1	195	8.32	0.0427	300	563
1	390	12.6	0.0324	600	855

Table C.13: MCR viscometer data of 0.1 weight% of titania-based mud at 25°C.

Meas. Pts.	Shear Rate	Shear Stress	Viscosity	Speed	Torque
-	[1/s]	[Pa]	[Pa·s]	[1/min]	[µNm]
1	1.95	1.67	0.855	3	113
1	3.9	2.13	0.547	6	144
1	65	10.1	0.155	100	680
1	130	17.1	0.131	200	1,160
1	195	23.7	0.122	300	1,610
1	390	42.4	0.109	600	2,870

Table C.14: MCR viscometer data of 0.1 weight% of titania-based mud at 50°C.

Meas. Pts.	Shear Rate	Shear Stress	Viscosity	Speed	Torque
-	[1/s]	[Pa]	[Pa·s]	[1/min]	[µNm]
1	1.95	1.41	0.723	3	95.3
1	3.9	1.77	0.454	6	120
1	65	6.49	0.0999	100	439
1	130	10.2	0.0787	200	692
1	195	13.7	0.0702	300	926
1	390	23.8	0.061	600	1,610

Table C.15: MCR viscometer data of 0.1 weight% of titania-based mud at 100°C.

Meas. Pts.	Shear Rate	Shear Stress	Viscosity	Speed	Torque
-	[1/s]	[Pa]	[Pa·s]	[1/min]	[µNm]
1	1.95	1.63	0.838	3	110
1	3.9	1.93	0.495	6	130
1	65	4.57	0.0703	100	309
1	130	6.18	0.0476	200	418
1	130	6.18	0.0476	200	418
1	390	11.4	0.0291	600	769

Table C.16: MCR viscometer data of 0.25 weight% of titania-based mud at 25°C.

Meas. Pts.	Shear Rate	Shear Stress	Viscosity	Speed	Torque
-	[1/s]	[Pa]	[Pa·s]	[1/min]	[µNm]
1	1.95	1.66	0.85	3	112
1	3.9	2.12	0.543	6	143
1	65	9.93	0.153	100	672
1	130	16.9	0.13	200	1,140
1	195	23.6	0.121	300	1,600
1	390	42.3	0.108	600	2,860

Table C.17: MCR viscometer data of 0.25 weight% of titania-based mud at 50°C.

Meas. Pts.	Shear Rate	Shear Stress	Viscosity	Speed	Torque
-	[1/s]	[Pa]	[Pa·s]	[1/min]	[µNm]
1	1.95	1.44	0.737	3	97.1
1	3.9	1.82	0.466	6	123
1	65	6.67	0.103	100	452
1	130	10.5	0.0809	200	711
1	195	14.1	0.0722	300	952
1	390	24.4	0.0627	600	1,650

Table C.18: MCR viscometer data of 0.25 weight% of titania-based mud at 100°C.

Meas. Pts.	Shear Rate	Shear Stress	Viscosity	Speed	Torque
-	[1/s]	[Pa]	[Pa·s]	[1/min]	[µNm]
1	1.95	1.7	0.872	3	115
1	3.9	1.95	0.501	6	132
1	65	4.77	0.0734	100	323
1	130	6.52	0.0502	200	441
1	195	7.98	0.041	300	540
1	390	12.1	0.031	600	816

Table C.19: MCR viscometer data of 0.5 weight% of titania-based mud at 25°C.

Meas. Pts.	Shear Rate	Shear Stress	Viscosity	Speed	Torque
-	[1/s]	[Pa]	[Pa·s]	[1/min]	[µNm]
1	1.95	1.76	0.901	3	119
1	3.9	2.31	0.592	6	156
1	65	11.1	0.17	100	748
1	130	18.8	0.145	200	1,270
1	195	26.1	0.134	300	1,760
1	390	46.2	0.119	600	3,130

Table C.20: MCR viscometer data of 0.5 weight% of titania-based mud at 50°C.

Meas. Pts.	Shear Rate	Shear Stress	Viscosity	Speed	Torque
-	[1/s]	[Pa]	[Pa·s]	[1/min]	[µNm]
1	1.95	1.5	0.771	3	102
1	3.9	1.84	0.472	6	125
1	65	6.82	0.105	100	462
1	130	10.7	0.0826	200	726
1	195	14.4	0.0738	300	973
1	390	24.9	0.064	600	1,690

Table C.21: MCR viscometer data of 0.5 weight% of titania-based mud at 100°C.

Meas. Pts.	Shear Rate	Shear Stress	Viscosity	Speed	Torque
-	[1/s]	[Pa]	[Pa·s]	[1/min]	[µNm]
1	1.95	1.7	0.871	3	115
1	3.9	1.98	0.508	6	134
1	65	4.76	0.0733	100	322
1	130	6.45	0.0497	200	437
1	195	7.89	0.0405	300	534
1	390	11.9	0.0305	600	804